AD NUMBER

AD474549

NEW LIMITATION CHANGE

TO

Approved for public release, distribution unlimited

FROM

Distribution authorized to U.S. Gov't. agencies and their contractors; Critical Technology; Sep 1965. Other requests shall be referred to Air Force Materials Lab., Attn: MAMD, Wright-Patterson AFB, OH 45433.

AUTHORITY

Air Force Materials Lab ltr dtd 12 Jan 1972

SECURITY MARKING

The classified or limited status of this report applies to each page, unless otherwise marked.

Separate page printouts MUST be marked accordingly.

THIS DOCUMENT CONTAINS INFORMATION AFFECTING THE NATIONAL DEFENSE OF THE UNITED STATES WITHIN THE MEANING OF THE ESPIONAGE LAWS, TITLE 18, U.S.C., SECTIONS 793 AND 794. THE TRANSMISSION OR THE REVELATION OF ITS CONTENTS IN ANY MANNER TO AN UNAUTHORIZED PERSON IS PROHIBITED BY LAW.

NOTICE: When government or other drawings, specifications or other data are used for any purpose other than in connection with a definitely related government procurement operation, the U. S. Government thereby incurs no responsibility, nor any obligation whatsoever; and the fact that the Government may have formulated, furnished, or in any way supplied the said drawings, specifications, or other data is not to be regarded by implication or otherwise as in any manner licensing the holder or any other person or corporation, or conveying any rights or permission to manufacture, use or sell any patented invention that may in any way be related thereto.

AFML-TR-65-269

MULTIPLE-BAND SURFACE TREATMENTS FOR HIGH D MPING

B. J. LAZAN, A. F. METHERELL and G. SOKOL

UNIVERSITY OF MINNESOTA

TECHNICAL REPORT AFML-TR-65-269

SEPTEMBER 1965

AIR FORCE MATERIALS LABORATORY
RESEARCH AND TECHNOLOGY DIVISION
AIR FORCE SYSTEMS COMMAND
WRIGHT-PATTERSON AIR FORCE BASE, OHIO

NOTICES

When Government drawings, specifications, or other data are used for any purpose other than in connection with a definitely related Government procurement operation, the United States Government thereby incurs no responsibility nor any obligation whatsoever; and the fact that the Government may have formulated, furnished, or in any way supplied the said drawings, specifications, or other data, is not to be regarded by implication or otherwise as in any manner licensing the holder or any other person or corporation, or conveying any rights or permission to manufacture, use, or sell any patented invention that may in any way be related thereto.

Copies of this report should not be returned to the Research and Technology Division unless return is required by security considerations, contractual obligations, or notice on a specific document.

400 - November 1965 - 14-274-773

MULTIPLE-BAND SURFACE TREATMENTS FOR HIGH DAMPING

B. J. LAZAN, A. F. METHERELL and G. SOKOL

UNIVERSITY OF MINNESOTA

FOREWORD

This report was written by the University of Minnesota, Department of Aeronautics and Engineering Mechanics, Minneapolis, Minnesota 55455, under USAF Contract No. AF 33(615)-1055, Project No. 7351, "Metallic Materials," Task No. 735106, "Behavior of Metals." The work was administered under the direction of Air Force Materials Laboratory, Research and Technology Division, with Mr. J. P. Henderson, MAMD, acting as project engineer.

The project was performed during the period from January, 1964 through July, 1965.

Manuscript of this report was released by the authors July 1965 for publication as an RTD Technical Report.

This technical report has been reviewed and is approved.

W. J. TRAPP
Chief, Strength and Dynamics Branch
Metals and Ceramics Division
Air Force Materials Laboratory

ABSTRACT

Conventional damping tapes, consisting of one or more adhesive layers constrained by relatively rigid bands, do not have sufficient damping for many applications. Considerable improvement can be realized in a multiple-band configuration in which alternate bands are rigidly anchored on opposite sides of the configuration. The energy dissipation in such a configuration is analyzed considering both short (rigid) bands and long (elastic) bands. General relations are derived between the configuration properties (in terms of the equivalent elastic modulus E_e' and the effective loss modulus E_e'') and a parameter which includes the material properties and the configuration geometry. Test configurations were made and tested. Experimental results are in excellent agreement with the theory. Both the theory and experimental results indicate that this new configuration is capable of dissipating very large damping energy, significantly higher than conventional surface treatments.

TABLE OF CONTENTS

ILLUSTRATIONS

ILLUSTRATIONS (CONT'D)

SYMBOLS

A^2 = a dimensionless parameter, which depends on the ratio of adhesive stiffness to band stiffness, $= G \ell^2/E^2 t^2 m$

B^2 = a dimensionless parameter = $|G^*| \ell^2/E_2 t_2 m$

D = unit damping energy dissipation in a material (in.-lb./cu. in.-cycle)

D_c = total damping energy dissipation in the surface treatment or configuration (in. lbs/cycle)

D_j = total damping energy dissipated in band-adhesive unit (in.-lb./cycle)

D_{jrb} = value of D_j for band-adhesive unit having rigid bands

E = modulus of elasticity of the band material (psi)

E^* = complex modulus of elasticity of the band (psi)

E' = storage (elastic) modulus of elasticity or Young's modulus of band (psi)

E'' = loss (out-of-phase) modulus of elasticity (psi)

E_e^* = $E_e' + i\, E_e''$
= equivalent complex modulus of elasticity of the configuration (psi)

E_e' = equivalent storage modulus of elasticity of the configuration (psi)

E_e'' = equivalent loss modulus of the configuration, the loss modulus of an equivalent uniform material which dissipates same energy (psi)

G^* = complex modulus of rigidity for a viscoelastic adhesive (psi)

G' = storage (elastic) modulus of rigidity (psi)

G'' = loss (out-of-phase) modulus of rigidity (psi)

H_x = $\cosh\left[\alpha\left(1 - \frac{x}{\ell}\right)\right] \cos\left[\beta\left(1 - \frac{x}{\ell}\right)\right]$

I_x = $\sinh\left[\alpha\left(1 - \frac{x}{\ell}\right)\right] \sin\left[\beta\left(1 - \frac{x}{\ell}\right)\right]$

J_w = $\cosh \alpha_w \cos \beta_w$

J_x = $\cosh \alpha \frac{x}{\ell} \cos \beta \frac{x}{\ell}$

k_j^* = $k_j' + i\, k_j''$

= complex modulus of the band-adhesive unit (lb./in.)

k_j' = the elastic modulus (ratio of in-phase component of the force to the displacement) of the band-adhesive unit (lb./in.)

k_j'' = the loss modulus (ratio of out-of-phase component of the force to displacement) of the band-adhesive unit (lb./in.)

k_{jrb}^*, k_{jrb}', and k_{jrb}'' are moduli for band-adhesive units having rigid (inextensible) bands

k_{jra}' = value of k_j' for band-adhesive unit having a rigid adhesive layer

k_c^* = $k_c' + i\, k_c''$

= complex modulus of the configuration (lb./in.)
Note: k_c' and k_c'' definition like those for k_j' and k_j''.

ℓ = length of a lap joint (in.)

L = distance between effective fixed points on ends of configuration

m = thickness of adhesive (in.)

M_w = $\alpha_w R_w - \beta_w S_w = \alpha_w \sinh \alpha_w \cos \beta_w - \beta_w \cosh \alpha_w \sin \beta_w$

M = $\alpha R - \beta S = \alpha \sinh \alpha \cos \beta - \beta \cosh \alpha \sin \beta$

n = number of band-adhesive units in a configuration

N_w = $\alpha_w S_w + \beta_w R_w = \alpha_w \cosh \alpha_w \sin \beta_w + \beta_w \sinh \alpha_w \cos \beta_w$

N = $\alpha S + \beta R = \alpha \cosh \alpha \sin \beta + \beta \sinh \alpha \cos \beta$

P_a = amplitude of sinusoidal force (lb.)

P_j = force in a band-adhesive unit (lb.)

Q_w = $\sinh \alpha_w \sin \beta_w$

Q_x = $\sinh \alpha \frac{x}{\ell} \sin \beta \frac{x}{\ell}$

R_w = $\sinh \alpha_w \cos \beta_w$

R = $\sinh \alpha \cos \beta$

S_w = $\cosh \alpha_w \sin \beta_w$

S = $\cosh \alpha \sin \beta$

t = time (sec.)

t_1 = thickness of adherend of modulus E_1 (in.)

t_2 = thickness of adherend of modulus E_2 (in.)

T_w = $(W^4 - 2W^2 + 2) J_w + (W^2 - 1)(M_w + 2)$

T = special value for T_w when W^2 is 2
= $2 \cosh \alpha \cos \beta + M + 2$

V_w = $(W^4 - 2W^2 + 2) Q_w + (W^2 - 1) N_w$

V = special value for V_w when W^2 is 2
= $2 \sinh \alpha \sin \beta + N$

W^2 = a convenient grouping of parameters = $1 + E_2 t_2 / E_1 t_1$

X_j = displacement in the band-adhesive unit (in.)

α_w = $WB \cos \delta/2$

α = special value for α_w when W^2 is 2
= $\sqrt{2}\, B \cos \delta/2$

β_w = $WB \sin \delta/2$

β = special value for β_w when W^2 is 2
= $\sqrt{2}\, B \sin \delta/2$

ψ_x = shear displacement in anelastic adhesive at any position x (in.)

ψ_o = ψ_x at $x = 0$

δ = phase angle by which the cyclic strain vector lags behind the cyclic stress vector during sinusoidal loading of a viscoelastic material = the loss angle

τ = shear stress in adhesive (psi)

γ = shear strain in adhesive

γ_a = amplitude of sinusoidal stress cycle

ω = frequency (radians per second)

η_j = loss coefficient of the band-adhesive unit

I. INTRODUCTION

High damping is often required in structural and machine members, particularly for those subjected to near-resonant excitation. In some cases high inherent damping in a structure can be attained by proper choice of materials or by design. In most cases, however, criteria other than damping generally determine material selection and design. Often, therefore, other means must be found for increasing damping. One method for accomplishing this is to utilize surface treatments which contain high damping viscoelastic adhesives.

In general, two types of surface treatments have been used for increasing the damping of a member. One is the viscoelastic coating, mastic or free layer (1,2,3) adhered to the surface, so that under cyclic loading the coating is subjected to the cyclic normal strains at the surface of the member. The second type is damping tape consisting of a viscoelastic damping adhesive and a constraining metal band which produce shear stress in the adhesive when the member surface to which it is attached is subjected to normal strains (2,3,4). In general, constrained layer or damping tape treatments are capable of higher damping than coating treatments (2,5,6).

A single such conventional damping tape often provides insufficient damping. For high damping multiple tapes such as shown in Figure 1 are sometimes employed. The surface treatment consists of several layers (four are shown in Figure 1) each having a thin metal band ("b" in Figure 1a) and a viscoelastic adhesive (shaded regions "a" in Figure 1a) which serves as the damping medium. For clarity in the Figure, the thickness in each band and of the adhesive layer is greatly exaggerated (normally they are a few thousandths of an inch thick). When the structural member is subjected to axial or bending load, normal strain is produced in the surface. This causes shear in the constrained viscoelastic adhesives as shown in Figure 1b. Under cyclic loading the adhesive layers are subjected to cyclic shear and they dissipate energy. Unfortunately, however, each successive band (No. 2, 3, 4, etc.) becomes less effective since the cyclic shear strains in the viscoelastic adhesive become progressively smaller ($c > d > e > f$, etc.). As a result, the additional damping realized by adding bands is generally limited. In fact, damping of multiple tapes is approximately equal to that of a single adhesive layer constrained by a metal band having a thickness equal to the sum of the individual band thicknesses (2).

Since conventional surface treatments do not provide sufficient damping for many types of applications, several new types of surface treatments have been developed (2,7,8). However, these new configurations are generally more complex and costly than the conventional treatments, generally more than can be justified by the higher damping realized.

A new type of multiple-band configuration for providing high damping in a surface treatment is described in this report, one which overcomes many of the limitations in prior treatments. The stress, strain, and damping analysis of this configuration and verifying experimental data are presented to demonstrate the high damping capacity of this new configuration.

II. ALTERNATELY ANCHORED, MULTIPLE-BAND TREATMENTS

One form of the new configuration is shown in Figure 2. Alternate bands are anchored on opposite ends of the configuration; that is, bands 1, 3, and 5 are rigidly attached to the structural member at location "p" (left side of surface treatment), and bands 2, 4, and 6 are attached at location "q" (right side). The viscoelastic adhesive (shaded regions) joins adjacent bands and provides the means for dissipating energy. The bands and adhesives are generally only a few thousandths of an inch thick (thickness greatly exaggerated in Figure 2), thus many layers can be included in the configuration.

Under cyclic axial or flexural loading the adhesive is subjected to cyclic shear (Figure 2b shows flexure loading). For this configuration, and unlike the multiple conventional damping tapes shown in Figure 1, the shear strain in successive adhesive layers is essentially the same irrespective of the number of layers. Thus, the damping of this surface treatment is approximately proportional to the number of bands, and is not limited in a manner observed for conventional multiple-band tapes. Therefore, the damping provided by the treatment can in theory be increased to the desired value.

The configuration shown in Figure 2 is suitable for beams or other members having uniaxial stress. Studies are now in progress on biaxial stress configurations for panels, plates, etc.

The alternately anchored band treatment has one disadvantage compared to the conventional damping tapes. Whereas in the conventional tapes the viscoelastic adhesive provides a means for attaching the surface treatment to the structural member, in the new configuration the bands must be rigidly anchored (using structural adhesives or other means of attachment) to the member at locations "p" and "q". The resultant stress concentrations at the attachment locations may require attention.

III. THE BAND-ADHESIVE UNIT AND ITS PROPERTIES

3.1 Definition of Band-Adhesive Unit and Assumptions.

Several bands and adhesive layers near band "j" located within the configuration are shown in Figure 3a. The entire configuration may

be considered to consist of band-adhesive units like the one indicated by the dashed line in Figure 3a and shown in Figure 3b. If all bands and adhesive layers have the same geometry and properties (in Figure 4a, $E_1 = E_2$, $t_1 = t_2$, and b and m are same for all layers*), then the band-adhesive unit lies between the midplanes of adjacent bands. If band thickness is "t" (see Figure 3a), then each band in the band-adhesive unit is t/2 thick (see Figure 3b). Under these circumstances all units are identical.

If band and adhesive geometry or properties varies with position j, then it becomes more difficult to define each unit. As a first approximation a unit might be considered to extend between planes of zero shear of adjacent band. In principle, therefore, it is possible to separate a configuration having unequal bands and adhesives into its component band-adhesive units, not all of which are necessarily equal.

The entire configuration contains n units (total number of bands is n, with n/2 mounted on each side, and the total number of adhesive layers is n). In general, the properties of the entire configuration may be determined from the properties of the band-adhesive units by a simple summation process. For example, total damping D_c of the configuration can be determined from the damping D_j of band-adhesive unit from:

$$D_c = \sum_{j=1}^{n} D_j \tag{3.1}$$

And if all band-adhesive units are equal, then:

$$D_c = n\, D_j \tag{3.2}$$

This section is concerned with the analysis of the band-adhesive unit and the entire configuration consisting of many such units is considered in Section IV.

The following assumptions are made in the analyses which follow.

(1) Bands and adhesive are very thin. Thus:
   (a) Bending effects in individual bands and adhesive layers can be neglected.
   (b) The adhesive layer is subjected to pure shear only (tension effects negligible).
   (c) The bands are subjected to pure tension only (shear effects negligible).

(2) The viscoelastic adhesive properties and the strain amplitudes considered are such that the damping remains linear (9). Under these circumstances complex

* See List of Symbols at beginning of report.

notation may be used to specify the unit properties of the adhesive material in terms of:

$$\tau = G' \gamma + \frac{G''}{\omega} \frac{\partial \gamma}{\partial t} \tag{3.3}$$

$$G^* = G' + i\, G'' \tag{3.4}$$

The damping energy dissipated per unit volume of adhesive material (in the linear range) is:

$$D = \pi\, G''\, \gamma_a^2 \tag{3.5}$$

(3) The thickness of the adhesive layer remains constant.

(4) The bands are elastic and dissipate no energy ($E'' = 0$ and $E = E^* = E'$).

(5) Poisson ratio effects are neglected and the one-dimensional problem only is considered.

The geometry and materials used in practical configurations and the large number of bands included generally justify these assumptions.

The significant properties of the band-adhesive unit can be specified in terms of the relations between the force P_j and the displacement X_j shown in Figure 3b. Since linear materials (in the viscoelastic sense) are assumed, complex notation is appropriate and the properties of the band-adhesive unit may be defined as:

$$k_j^* = k_j' + i\, k_j'' \tag{3.6}$$

The loss coefficient of the unit is:

$$\eta_j = k_j''/k_j' \tag{3.7}$$

The damping energy dissipated per cycle of displacement amplitude X_a or per cycle of force amplitude P_a is:

$$D_j = \pi\, k_j''\, X_a^2 = \pi \frac{k_j''}{k_j'^2}\, P_a^2 = \pi \frac{\eta_j}{k_j'}\, P_a^2 \tag{3.8}$$

3.2 Theory and Experimental Results for Band-Adhesive Unit Having Unequal Bands (Width Constant).

For generality we consider first the case of unequal bands having thickness t_1 and t_2 and stiffness E_1 and E_2 as shown in Figure 4a. The two bands are connected by a layer of adhesive of thickness "m". In this section we consider two cases (a) an elastic adhesive having

a conventional shear modulus ($G' = 0$ and $G = G^* = G'$), and (b) a viscoelastic adhesive having a loss coefficient G''.

3.2a Limiting Cases.

As the first limiting case we consider bands that are rigid or inextensible in comparison to the adhesive layer (E is infinitely large, yet bands are still assumed to be flexible in bending). Under these circumstances the shear strain in the adhesive layer is uniform. If the dimensions of the adhesive layer are m, b, and ℓ as shown in Figure 4, the relationship between the unit properties of the adhesive and the properties of the band-adhesive unit having rigid bands (subscript "rb" added to designate "rigid band" theory) are:

$$k^*_{jrb} = G^* (\ell\ b/m)$$
$$k'_{jrb} = G' (\ell\ b/m)$$
$$k''_{jrb} = G'' (\ell\ b/m) \qquad (3.9)$$
$$D_{jrb} = \pi\, k''_{jrb}\, X_a^2 = \pi \frac{k''_{jrb}}{k'^2_{jrb}}\, P_a^2$$

As a second limiting case we consider the adhesive layer to be very rigid ($G' = \infty$ and $G'' = 0$) compared to the bands. Under these circumstances the properties of the band-adhesive unit are simply those of a band having a thickness equal to $t_1 + t_2$ and a length ℓ. Using the subscript "ra" to designate the "rigid adhesive" theory:

$$k'_{jra} = E\, b(t_1+t_2)/\ell \qquad (3.10)$$

3.2b Units Having Elastic Band and Elastic Adhesive.

In most practical applications significant strain occurs in the bands and adhesive. Thus, neither the rigid band theory (and the associated uniformity of shear strain in the adhesives) nor the rigid adhesive theory described above is appropriate. We discuss first the case of the elastic bands ($E'' = 0$ and $E^* = E' = E$) and elastic adhesive ($G'' = 0$ and $G^* = G' = G$).

The elastic constant of the unit is $k_j = P_j/X_j$, where the displacement caused by force P_j is, from Figure 4b:

$$X_j = \psi_o + e_1 \qquad (3.11)$$

where $\psi_o = (\psi_x)_{x=0}$ = shear displacement in the adhesive at $x = 0$. (in.)

e_1 = total extension in band 1. (in.)

The values of ψ_o and e_1 are derived below.

The shear displacement ψ_s in the adhesive at section x is (10,11)

$$\psi_x = \frac{P_j A m}{W b \ell G \sinh WA} \left[(W^2-1)\cosh(WA\,\tfrac{x}{\ell}) + \cosh WA\,(1 - \tfrac{x}{\ell})\right] \qquad (3.12)$$

where: $A^2 = G\,\ell^2/E_2 t_2 m$ (3.13)

= dimensionless ratio of adhesive stiffness to band stiffness

$$W^2 = (E_1 t_1 + E_2 t_2)/E_1 t_1 \ . \qquad (3.14)$$

And at x = 0 the shear displacement is:

$$\psi_o = (\psi_x)_{x=0} = \frac{P_j A m}{W b \ell G \sinh WA} \left[(W^2-1) + \cosh WA\right] . \qquad (3.15)$$

To determine e_1 we consider the force P_x at section x in band 1.

$$P_{1x} = \int_0^x b\,\tau_x\,dx \qquad (3.16)$$

where: τ_x = the adhesive shear stress at any position $x = G\,\psi_x/m$.

The force and unit strain in the band 1 at section x are:

$$P_{1x} = \frac{bG}{m} \int_0^x \psi_x\,dx \qquad (3.17)$$

$$e_{1x} = \frac{G}{E_1 t_1 m} \int_0^x \psi_x\,dx \ . \qquad (3.18)$$

Substituting for ψ_x (Eq. 3.12) and integrating from 0 to x:

$$e_{1x} = \frac{P_j}{W^2 E_1 t_1\, b \sinh WA} \left[(W^2-1)\sinh WA\,\tfrac{x}{\ell} - \sinh WA\,(1 - \tfrac{x}{\ell}) + \sinh WA\right]. \qquad (3.19)$$

The total extension e_1 of band 1 is:

$$e_1 = \int_0^\ell e_{1x}\,dx.$$

Substituting Equation (3.19) and integrating:

$$e_1 = \frac{(W^2-1)\ m\ P_j\ A}{W^3 b \ell G \sinh WA}\left[(W^2-2)(\cosh WA-1) + WA \sinh WA\right]. \qquad (3.20)$$

Substituting Equations (3.20) and (3.15) in (3.11) the total or overall extension of the band-adhesive unit (see Figure 4b) is:

$$X_j = \frac{\ell P_j \left[(W^4-2W^2+2)\cosh WA + (W^2-1)\ (2 + WA \sinh WA)\right]}{W^2 b\ E_2 t_2\ WA \sinh WA} \qquad (3.21)$$

Thus the elastic constant of the completely elastic band-adhesive unit ($k_j'' = 0$ and $k_j^* = k_j' = k_j$) is:

$$k_j = \frac{P_j}{X_j}$$

$$= \frac{W^2\ b\ E_2 t_2\ WA \sinh WA}{\ell\left[(W^4 - 2W^2+2)\cosh WA + (W^2-1)\ (2 + WA \sinh WA)\right]} \qquad (3.22)$$

3.2c Units Having Elastic Bands and Viscoelastic Adhesives.

We consider next the case where the adhesive layer is assumed to be viscoelastic ($G^* = G' + i\ G''$). The equations for this case can be derived by proceeding as for the elastic case discussed above except by replacing the conventional elastic modulus G by the complex modulus $G^* = G' + i\ G''$. Defining $\tan \delta = G''/G'$ and $B^2 = G^*\ \ell^2/E_2 t_2 m$ the following substitutions can be made.

$$WA = WB\ (\cos \delta/2 + i \sin \delta/2) = (\alpha_w + i\ \beta_w)$$

$$\cosh WA = \cosh \alpha_w \cos \beta_w + i \sinh \alpha_w \sin \beta_w = J_w + i\ Q_w$$

$$\sinh WA = \sinh \alpha_w \cos \beta_w + i \cosh \alpha_w \sin \beta_w = R_w + i\ S_w$$

Using these substitutions, Equation (3.22) becomes

$$k_j^* = \frac{P_j^*}{X_j} = \frac{W^2 b E_2 t_2}{\ell}\ \frac{(\alpha_w + i\ \beta_w)\ (R_w + i\ S_w)}{\left\{(W^4-2W^2+2)(J_w+iQ_w)+(W^2-1)\left[(\alpha_w+i\beta_w)(R_w+iS_w)+2\right]\right\}}$$

$$= \frac{W^2 b E_2 t_2}{\ell}\ \frac{(M_w T_w + N_w V_w) + i\ (N_w T_w - M_w V_w)}{T_w^2 + V_w^2} \qquad (3.23)$$

The components of the complex modulus can be determined by equating the real and imaginary parts of Equations (3.6) and (3.23).

$$k_j' = \frac{W^2 b E_2 t_2}{\ell} \quad \frac{(M_w T_w + N_w V_w)}{(T_w^2 + V_w^2)} \tag{3.24}$$

$$k_j'' = \frac{W^2 b E_2 t_2}{\ell} \quad \frac{(N_w T_w - M_w V_w)}{(T_w^2 + V_w^2)} \tag{3.25}$$

$$\eta_j = \frac{k_j''}{k_j'} = \frac{N_w T_w - M_w V_w}{M_w T_w + N_w V_w} \tag{3.26}$$

3.2d Experimental Results and Comparison with Theory.

Test results by Avery (11) on a number of double unit configurations are given in Figure 5 (schematic diagram of test set-up is given in insert in Figure 5). Various adherend materials and thicknesses were used to adjust the values of E_2t_2 to cover the range between the rigid band theory (see Equations 3.9) and the rigid adhesive theory. The adhesive used was 3M #466 (at test frequency of 0.25 cyps, $G^* = 7$ and $\eta = 0.4$). All test data are for $W = 1$ ($E_1t_1 = \infty$). Avery's test results and the theoretical curve for this case (see Equations 3.8, 3.25 and 3.26) are compared in Figure 5, using parameter B as a basis for comparison. The check between theory and the experimental data is excellent except at the high values of B. In the rigid adhesive range (high values of B) highly non-homogeneous shear occurs in the adhesive (see Figure 6c for case of $W^2 = 2$ as example) and the high localized shear in the adhesive can cause adhesive separation, thus reducing the observed damping.

These comparisons are made on the basis of damping at a specified force amplitude, in which case dimensionless damping increases with B. If comparisons are made on the basis of damping at a specific displacement (or on the basis of dimensionless loss modulus) as discussed in the next section, a decrease is observed with increasing values of parameter B.

3.3 Theory of Band-Adhesive Unit Having Viscoelastic Adhesive and Equal Bands ($W^2 = 2$).

If the bands are equal ($E_1t_1 = E_2t_2 = E(t/2)$ as shown in Figure 6), then $W^2 = 2$. Under these circumstances it can be shown (10) that the shear strain in the adhesive is:

$$\gamma_x = P_a^m \frac{0.71\ B}{b\ \ell\ |G^*|} \frac{\Lambda}{\Omega} \tag{3.27}$$

where $\Lambda = \left[H_x^2 + I_x^2 + 2\,(H_xJ_x + I_xQ_x) + J_x^2 + Q_x^2\right]^{\frac{1}{2}}$

$$\Omega = \left[R^2 + S^2\right]^{\frac{1}{2}}$$

Defining ψ_{rbf} as the uniform shear strain displacement for the rigid band case under a specified <u>force</u> amplitude P_a, $\psi_{rbf} = \frac{P_a m}{bt\,|G^*|}$, and:

$$\frac{\psi_x}{\psi_{rbf}} = 0.71\ B\ \frac{\Lambda}{\Omega} \tag{3.28}$$

Defining ψ_{rbd} as the uniform shear strain displacement for the rigid band case under a specified <u>displacement</u> amplitude $X_a = P_a/k_j' = \psi_{rbd}$, and:

$$\frac{\psi_x}{\psi_{rbd}} = \frac{k_j'}{G^*}\ \frac{mB}{bt}\ \left(0.71\ \frac{\Lambda}{\Omega}\right) = \frac{k_j'}{k_{jrb}'}\ \left(0.71\ B\ \frac{\Lambda}{\Omega}\right)\cos\delta \tag{3.29}$$

And from Equation (3.27)

$$\frac{\psi_x}{\psi_{rbd}} = \left(\frac{k_j'}{k_{jrb}'}\right)\left(\frac{\psi_x}{\psi_{rbf}}\right)\cos\delta \tag{3.30}$$

The properties of the band-adhesive unit in terms of its complex moduli and its loss coefficient can be determined by substituting $W^2 = 2$ in Equations (3.24), (3.25), and (3.26).

$$k_j' = \frac{bEt}{t}\ \frac{MT + NV}{T^2 + V^2} \tag{3.31}$$

$$k_j'' = \frac{bEt}{t}\ \frac{NT - MV}{T^2 + V^2} \tag{3.32}$$

$$\eta_j = \frac{NT - MV}{MT + NV} \tag{3.33}$$

Curves illustrating the shear strain distribution for a particular case ($\eta = 0.40$ and $G^* = 7$ psi) for three values of parameter B are shown in Figure 6. Distance along the ordinate scale is made proportional to the fourth root of the ordinate value to spread out

curves and avoid crowding near zero. Both the specified force amplitude case (Ψ_{rbf}) and the specified displacement amplitude cases (Ψ_{rbd}) are illustrated.

Under a specified force amplitude (dashed lines in Figure 6) the localized strain at the ends of flexible bands may be much larger than for the rigid band case (for B = 10 it is about seven times as large). Since the effective strain amplitude from a damping viewpoint is the root-mean-square strain ($D_x \alpha \Psi_x^2$), the D_j of the extensible band configuration is larger than for the rigid band case (see Figure 9 discussed later).

The ratio Ψ_x/Ψ_{rbd}, under a specified displacement amplitude, can be determined from Ψ_x/Ψ_{rbf} by using the multiplying factor k'_j/k'_{jrb} as shown by Equation (3.30). This dimensionless storage modulus is never larger than unity and may be very small (see Figure 7). As shown in Figure 6, the localized shear displacement is never larger than that in the rigid band and is generally much smaller. Thus, the damping is always smaller for the flexible band case than for the rigid band case, very much smaller in some cases.

The general damping and stiffness properties of the band-adhesive unit are defined in Equations 3.31, 3.32, and 3.33. The important trends revealed by these equations are shown graphically in Figures 7, 8, 9, and 10 in which a dimensionless property is plotted against parameter B, where B is a dimensionless ratio of the adhesive stiffness to the band stiffness.

The ordinate used in Figure 7 is the storage modulus k'_j of the unit, made dimensionless by dividing by k'_{jrb} of the rigid band unit. Up to a value B of approximately 0.3, the dimensionless storage modulus is constant, indicating that the rigid-band equations are appropriate in this region. At the other extreme, at values of parameter B greater than 5, the storage modulus is equal to that of a solid member without joints (the rigid adhesive region). The intermediate region, one in which many practical configurations lie, is the transition region between the rigid band and the rigid adhesive behavior and includes characteristics of both types.

The storage modulus is not only dependent on parameter B but also on the loss coefficient η. However, η does not affect the dimensionless modulus critically. In fact, the curves for η between 0 and 0.2 are practically identical as shown in Figure 7, and the curve for $\eta = 1.0$ lies about 30 per cent above $\eta = 0.2$ curve.

The loss modulus k''_j of the band-adhesive unit, made dimensionless by dividing by the rigid-band value k''_{jrb}, is shown in Figure 8 as a

function of parameter B. The general character of the relationship shown is similar to that for the storage modulus given in Figure 7 and a rigid-band region, etc. can be identified. Since k''_j is the proportionality constant between the damping energy dissipated and the square of the displacement amplitude (see Equation 3.8), Figure 8 indicates directly the reduction in damping at a specified displacement from that for the rigid-band theory as B is increased. At a value B = 1 the effective loss modulus is about half of that predicted by rigid-band theory, and at B = 5 the reduction to about 1% of the rigid-band value. The physical reason for this may be seen from Figure 6; under a specified displacement the effective (rms) strain distribution is smaller and thus the damping is smaller.

In contrast with the reduction observed in the dimensionless loss modulus with increasing parameter B, the damping energy dissipated at a specified force amplitude may increase significantly with B as shown in Figure 9. This increase is associated with the high strain amplification at the ends of the bands (see Figure 6c), and a similar trend was illustrated in Figure 5.

Finally, the loss coefficient η_j of the configuration, made dimensionless by dividing by the loss coefficient η_{jrb} for the rigid-band configuration, decreases with increasing values of parameter B as shown in Figure 10.

Figures 7 through 10 show that significant differences are observed between the properties of the rigid-band configuration and those having flexible bands in the range of engineering interest. The combinations of material properties and configuration geometry which characterize practical treatments cover the range of B from 0.1 to probably over 100. The figures show that in this range many of the important dimensionless properties vary up to over two orders of magnitude.

IV. PROPERTIES OF THE MULTIPLE-BAND CONFIGURATION IN TERMS OF $k^*_j = k'_j + i\, k''_j$ OF THE TYPICAL BAND-ADHESIVE UNIT

The properties of the configuration may be expressed in two ways. One approach is in terms of its overall complex modulus $k^*_c = k'_c + i\, k''_c$. the second method is to determine the equivalent complex modulus $E^*_e = E'_e + i\, E''_e$ for a volume equal to that of the entire configuration. These two approaches are reviewed in this Chapter.

4.1 Properties in Terms of $k_c^* = k_c' + i\, k_c''$.

4.1a Uniformly Strained Configurations.

If the member to which the configuration is attached is subjected to pure axial strain or if the configuration is very thin compared to the member, then the extension X_j is the same for each band-adhesive unit ($X_1 = X_n$ in Figure 11). The properties of the entire configuration may, in general, be determined from the properties of the band-adhesive units by a simple summation process. Thus:

$$k_c^* = \sum_{j=1}^{n} k_j^* \tag{4.1}$$

However, in the actual damping configuration considered all band-adhesive units are reasonably constant in geometry and properties. Under these circumstances $k_{j-1}^* = k_j^* = k_{j+1}^* = k_{j+2}^*$, etc. and $D_{j-1} = D_j$, etc. Thus, k_j^* and D_j^* may be considered to be the properties of the typical band-adhesive unit. Bands and adhesives near the member surface or near the free surface of the configuration will have somewhat different stress and strain distributions than those near the middle (typical) ones. However, the configuration is assumed to have many bands, therefore, the atypical character of the few surface bands is generally not significant.

For cases where analysis in terms of the typical band-adhesive unit (see Figure 3b) is appropriate each band has a force $2P_j$ and a displacement X_j. Since n/2 bands are attached to each side (see Figure 3a), Equations (4.1) reduce to

$$k_c^* = \sum_{j=1}^{n} k_j^* = \left(\frac{n}{2}\right) \frac{2P_j}{X_j} = n\, k_j^* \tag{4.2}$$

$$k_c' = n\, k_j'$$

$$k_c'' = n\, k_j''$$

Expressed in terms of damping energy the properties of the configuration are:

$$D_c = \pi\, k_c''\, X_a^2 = \pi\, n\, k_j''\, X_a^2 \tag{4.3}$$

The resultant force on the configuration is located at the middle band (in Figure 11, $g = d/2$).

4.1b Non-Uniformly Strained Configurations.

If the surface treatment is not thin compared to the member to which it is attached, the bands are generally subjected to different strains (see example of flexure illustrated in Figures 2b and 11). In this case Equations (4.2) are not appropriate. The equations for the "thick" treatment case, considering the non-uniform strain distribution, are derived below.

A thick treatment is shown attached to a beam in Figure 11. The minimum total strain X_1 exists at band 1 (located at the bear surface) and the maximum is X_n located at the outermost band. The distribution of forces P_j in the band-adhesive units and the resultant P_c of these forces are shown in Figure 11. Assuming a large number of bands* and assuming the band numbering shown in Figures 2 and 3:

$$P_c = 2P_1 + 2P_3 + 2P_5 + \text{---} + 2P_n$$

Considering all band-adhesive units are identical:

$$P_c = 2k'_j \left[X_1 + X_3 + X_5 + \text{---} + X_n\right]$$

$$= 2k'_j \left[\frac{n}{2}\left(\frac{X_1+X_n}{2}\right)\right] = \left(\frac{n}{2}\right) k'_j X_1 \left(\frac{X_n}{X_1} + 1\right) \qquad (4.4)$$

The location of this resultant force, as given by distance g from the surface of the beam (see Figure 11), is:

$$g = \frac{d}{3}\left(\frac{X_1}{X_n} + 2\right) \Big/ \left(\frac{X_1}{X_n} + 1\right) \qquad (4.5)$$

The strain X_c at this location is:

$$X_c = X_1\left[1 + \frac{c}{d}\left(\frac{X_n}{X_1} - 1\right)\right]$$

$$\frac{X_c}{X_1} = 1 + \left[\frac{1}{3}\left(\frac{X_1}{X_n} + 2\right)\left(\frac{X_n}{X_1} - 1\right) \Big/ \left(\frac{X_1}{X_n} + 1\right)\right] \qquad (4.6)$$

* If n is small, then consideration must be given to whether n is even or odd. To simplify the derivations given below n is assumed to be odd.

The elastic constant k'_c of the treatment may now be defined in terms of the ratio of the total (or resultant) force P_c in the treatment to the displacement X_c at the location of the resultant forces. Thus:

$$k'_c = \frac{P_c}{X_c} = \frac{n}{2}\, k' \, \frac{\left(\frac{X_n}{X_1} + 1\right)}{1 + \left[\frac{1}{3}\left(\frac{X_1}{X_n} + 2\right)\left(\frac{X_n}{X_1} - 1\right) \Big/ \left(\frac{X_1}{X_n} + 1\right)\right]} \tag{4.7}$$

The effects of the surface addition on the stiffness of the beams can be determined by assuming a spring constant k'_c given by Equation (4.7) located at a distance "g" (Equation 4.5) from the beam surface and attached at points p and q a distance "L" apart. Distance "L" is greater than "ℓ" by a distance governed by the geometry of the attachment ends (see Figure 11).

The loss modulus k''_c for the entire configuration can be determined from the damping energy dissipated by the surface treatment. The total damping is the sum of that contributed by all n units, thus

$$D_c = \sum_{j=1}^{n} D_j \tag{4.8}$$

If the typical unit approach is appropriate, then from Equation (3.5)

$$\begin{aligned} D_c &= \pi\, k''_j\, (X_1^2 + X_2^2 + X_3^2 + \text{---} + X_n^2) \\ &= \pi\, n\, k''_j \left[\frac{\Sigma\, X_n^2}{n}\right] = \pi\, n\, k''_j\, X_{rms}^2 \end{aligned} \tag{4.9}$$

where X_{rms} = "root-mean-square" displacement

$$= X_1 + 0.707\,(X_n - X_1) \tag{4.10}$$

If the loss modulus k''_c of the entire configuration is defined in terms of the root-mean-square displacement as given by Equation (4.10), then:

$$D_c = \pi\, k''_c\, X_{rms}^2 \tag{4.11}$$

From Equations (4.9) and (4.11)

$$k''_c = n\, k''_j \tag{4.12}$$

4.2 Configuration Properties in Terms of Its Equivalent Complex Moduli $E^*_e = E'_e + i\, E''_e$.

In many cases the surface strain in the member is reasonably uniform over the length where the surface treatment is attached (vibration wave length much larger than the treatment length). To analyze such cases it is often convenient to consider the effects of a configuration added to a surface of a member in terms of (or by replacing it by) a homogeneous material having (a) the same cross-sectional area and length L, and (b) attached to the member over distance "L" (see Figure 11). The effects of the treatment can then be considered in terms of the equivalent moduli E'_e and E''_e such that the homogeneous equivalent material has the same overall stiffness and damping properties as the configuration. The values of E'_e and E''_e for the equivalent homogeneous material are derived next.

The overall elastic constant k'_c of the homogeneous material (see Equation 4.2) having the same volume and attached at points p and q (distance L apart) as the configuration is:

$$k_c = E'_e \left(\frac{bd}{L}\right) = n\, k'_j$$

$$\text{Thus:} \quad E'_e = n\, k'_j\, (L/bd) = k'_j\, (L/bh) \tag{4.13}$$

where: h = total thickness of band-adhesive unit = m + t.

The loss modulus E''_e of the equivalent homogeneous material must be such that the same energy dissipation as the configuration. Since $D = \pi\, E''\, \epsilon_a^2$ (see Equation 3.3) and from Equation (4.3),

$$D_c = \pi\, E''_e\, \epsilon^2\, (bdL) = \pi\, n\, k''_j\, X_j^2$$

but $\epsilon = X_j/L$, thus:

$$E''_e = n\, k''_j\, (L/bd) = k''_j\, (L/bh) \tag{4.14}$$

The equivalent loss coefficient is:

$$\eta_e = \frac{E''_e}{E'_e} = \frac{k''_j}{k'_j} \tag{4.15}$$

V. TEST CONFIGURATION, EXPERIMENTAL RESULTS AND COMPARISON WITH THEORY

5.1 Description of Multiple-Band Configuration Used in Test Program and Its Predicted Properties.

The test configuration used in the experimental verification program is shown in Figure 12. For clarification the vertical scale is about 50 times larger than the horizontal scale. The total thickness of the configuration is only 0.04" as compared with its overall length of 6 inches. Bands were steel, for which $E = 30 \times 10^6$. For the adhesive used for the damping layer (No. 466 manufactured by Minnesota Mining and Manufacturing Co.), $G' = 15.5$ psi and $G'' = 13.2$ psi at the frequency of 0.78 cps and at room temperature used in the test program.

The main bands in the configuration are identified as 1 through 5, and the damping adhesive is shown by the shaded layers between the bands. The configuration was assembled by progressively building up layer upon layer by applying the damping adhesive as illustrated and structural adhesive (Scotch Weld EC 2158 manufactured by Minnesota Mining and Manufacturing Co.) at interfaces f. To simplify construction bands having constant cross-section are used and spacer sheets inserted between bands as shown to produce the desired geometry. After the configuration is assembled, it may be attached to the member surface using structural adhesives at interfaces g-h and w-y and using damping adhesive in the middle region h-w.

In order to maximize the damping of the configuration per unit weight or size, it is often necessary to use thin bands (0.006" thickness used in the test configuration). At the same time it is necessary to provide sufficient clearance at the ends of the bands to accommodate shear strain in the adhesive without contact between band ends and spaces (see regions r and r' in Figure 12). This leaves a short length of band unsupported by the adhesive and buckling may require consideration in some cases. One approach for minimizing the possibility of buckling is through careful geometry control. Generally only a few thousandths of an inch is required for clearance for adhesive shear motions, and thus the minimum unsupported length of band is generally smaller than the band thickness. Thus, with careful dimension control, buckling possibilities can be minimized. Another approach is to stagger the unsupported section of alternate bands as shown by the displacement between r and r', so that each band is supported by adhesive on at least one side over its entire length.

Another approach for minimizing buckling and maximizing damping is to utilize bands which taper towards their free end within a configuration (constant stress member approach). The use of tapered bands also allows including more bands per given space for a given band stiffness. Theoretical and experimental studies on tapered bands are now in progress.

Of the several possibilities the staggered gap approach was used in the test configuration investigated in this program.

To simplify the analysis of the test configuration, only four active damping adhesive layers were considered (between bands 1 and 2, 2 and 3, 3 and 4, and 4 and 5). The damping adhesive between band 1 and the member surface is also subjected to cyclic shear, but the magnitude is much smaller than in the active bands; therefore, it was not considered in the analysis (estimated energy dissipated by the damping layer between band 1 and the member surface is about 10% of that in the active damping adhesive layer).

Even though the test configuration has very few bands, and the length of each band is somewhat different, nevertheless the typical band-adhesive unit approach discussed in Section 3.3 was used in predicting the properties of the test configuration. The properties k'_j and k''_j of the typical band-adhesive unit for the particular values of material and geometry properties for the test configuration are shown in Figure 13 as a function of length ℓ of configuration. The rigid-band theory and the rigid-adhesive theory are shown as straight lines in Figure 13, and these correspond to similar straight lines shown in Figure 7 for the more general curves. The experimental points included in Figure 13 are discussed later.

As mentioned previously, the concept of an equivalent storage modulus, loss modulus and loss coefficient of a uniform homogeneous material provides a useful practical approach for analyzing the effect of the surface treatment. Theoretical values for these equivalent properties are shown in Figure 14. These values are based on the assumption that the end-connections of the configuration are such that the anchor length L (see Figure 11) is 1 inch longer than the adhesive length ℓ. These theoretical curves show that the maximum value of E''_e (at an optimal length ℓ of about 3") is very high indeed, approximately 4,000,000 psi. This is one or two orders of magnitude higher than currently available homogeneous viscoelastic materials. At the same time the storage modulus E'_e is also very high, over 10^6 psi in the region of engineering interest.

5.2 Test Procedure, Vibration Decay Results, and Observed Values of Moduli k'_j and k''_j.

A vibration decay method was used to determine experimentally the damping properties of the configuration. Measurements for determining the storage modulus k'_j of the configuration were not made.

The test beam to which the multiple-band configuration is attached and the test apparatus are shown in Figure 15. A tapered beam was used so that under the moment distribution imposed during the vibration test the surface strain is uniform over the region to which the configuration is attached. An extension arm and weight are

attached to the beam and the whole assembly mounted vertically. To perform a test the mass at the lower end of the lower beam is displaced and released. Measurements on amplitude of vibration are then made as a function of time during decay (natural frequency of vibration is about 0.78 cycles per second).

The decay test results are shown in Figure 16 in terms of dimensionless amplitude, the ratio of the amplitude at any number of cycles divided by that amplitude associated with zero cycles. As shown in Figure 16 the decay process is linear; thus, the particular amplitude associated with the zero cycle is immaterial.

Two different lengths were used for the test configurations. By stripping off layers the number of band-adhesive units tested was four, two, and one.

The effectiveness of the surface treatment is apparent from Figure 16. The test system used stores considerable strain and potential energy during displacement. The test beam is 3/16" thick, 1.6" wide, and 7" long; thus, it is capable of storing considerable strain energy. In addition, the extension arm and attached weight behave like a pendulum (see Figure 19) and the potential energy associated with the elevation of its center of gravity is approximately 80% of the strain energy stored in the beam. Nevertheless, the surface treatment produced the very large increase in decay rate observed in Figure 16. If a thinner test beam or a lighter pendulum were used, the change in logarithmic decrement caused by the surface treatment would be even more dramatic; and if thicker beams were used, a smaller change in log decrement would be observed.

These methods were used to compare the experimental results with the values predicted by the theory developed in the previous sections.

First, the log decrement data shown in Figure 16 was converted to values of the loss modulus using the analytical methods detailed in Appendix A. This led to the values for k''_j shown as the three points in Figure 13. The experimental points fall within about 15% of the theoretical curve. Considering variability in properties and other test uncertainties, this check is considered excellent. Tests were also performed on a single band unit having a $\ell = 2$, and this point (not shown in Figure 13) fell 33% above the theoretical curve. However, as mentioned previously, the computation did not include the damping energy dissipated in the damping layer between band 1 and the beam surface (see Figure 12). Furthermore, the atypical character of the end bands was not considered. These factors, if considered, would bring the theory and experimental results even closer.

In the second method used the equivalent loss modulus E''_e (see Section 4.2) was computed and used to determine the overall loss coefficient η_s of the experimental system. The values predicted by this

theory are shown in Table I, Column (b). These compare favorably with the experimental values for η_s shown in Table I, Column (a). These experimental values for the treated beams were determined directly from the Δ_t data shown in Figure 16, subtracting in each case the damping not due to the treatment (that caused by the beam, grip and machine losses) as represented by the "no treatment" curve on Figure 16.

The methods discussed above utilize the concept of a typical band. However, each band in the test configuration had a somewhat different length ℓ. To avoid this approximation a third method was used to make layer-to-layer summation (using equations of type 3.1). Approximate summation methods considering the actual length of each adhesive layer and the band geometry factors on each side of the adhesive layer (band location and position factors, particularly with reference to the outer bands). Theoretical values of η_s so determined are given in Table I, Column (c). Although this method leads to an improved check with theory, it is more awkward and time-consuming to use than the theories associated with the typical unit band concept.

All three methods confirm the validity of the theory, at least in the range of measurements. Additional tests are planned to compare theory and experiment for lengths remote from the optimum length for maximum loss modulus.

VI. COMPARISONS WITH CONVENTIONAL FREE AND CONSTRAINED LAYER TREATMENTS

Many factors must be considered in comparing the effectiveness of the new configurations and treatments with conventional damping treatments. Beyond its damping capacity the weight, cost, ease of use, and durability of treatment must be considered. However, in many applications a comparison on the basis of equal weight of surface treatment is appropriate. Kerwin and Ungar (2,5) have used this type of comparison. Different types of treatments are rated in Figure 17 in terms of the maximum loss coefficient versus the ratio of the treatment related to the weight of the base plate. The comparisons between the free layer* and the constrained layer treatment (curves a and b) are taken from references 2 and 5. The uppermost curve shown as "c" in this Figure indicates the possibility offered by the new alternately anchored multiple-band treatment. Curves c were constructed

* The values of E" used in Figure 17 for comparison purposes are identified as typical values (5). However, free layer materials recently described have higher values of E". For example, material LD-400 manufactured by Lord Mfg Co. has an E" higher than 100,000 psi, and for this value the free-layer curve would lie in the vicinity of the conventional layer curves (b) in Figure 17.

directly from the free-layer curves (a) by considering loss moduli and specific gravity ρ ratios. The particular multiple-band treatment represented in this Figure is not necessarily the maximum value attainable; it is merely the maximum value for rather arbitrarily selected band and adhesive thicknesses and other geometry features. Nevertheless, the new configuration when compared on this basis is approximately an order of magnitude more effective than conventional treatments for treatment weights less than 10% of the plate weight.

To indicate the effectiveness of the new treatment as compared with conventional treatments the loss coefficient of the actual test beam with conventional damping tapes was computed. Assuming that an infinite number of conventional damping tapes are applied to the test beam (and approximating its effect to be equivalent to one band having $E_3 t_3 = \infty$ with a single adhesive layer (2)), and assuming negligible shift in the neutral axis:

$$\psi_x = \frac{x}{\rho} \frac{h}{2} = \frac{xhy_e}{49} \tag{6.1}$$

The damping energy dissipated by the damping tape is:

$$D_c = 2 \int_0^{\ell/2} \pi G'' \left[\frac{xhy_e}{49\ m}\right]^2 m\ b\ dx = \frac{\pi G''\ b\ h^2 \ell^3 y_e^2}{28800\ m} \tag{6.2}$$

Using the methods detailed in Appendix A, the following comparisons can be made.

For $\ell = 2''$.

Conventional tape with $n = \infty$, $\eta_s = 0.00033$
New configuration with $n = 4$, $\eta_s = 0.031$
New configuration with $n = 10$, $\eta_s = 0.0873$

For $\ell = 4''$.

Conventional tape with $n = \infty$, $\eta_s = 0.0026$
New configuration with $n = 2$, $\eta_s = 0.028$
New configuration with $n = 10$, $\eta_s = 0.0868$.

VII. CONCLUSIONS

The theory developed for the alternately anchored multiple-band surface treatment provides a convenient method for predicting its stiffness and damping properties. These may be represented in terms

of two types of units: - (a) the storage modulus k'_c, loss modulus k''_c and loss coefficient η_c of the configuration, or (b) the equivalent storage modulus E'_e and the loss modulus E''_e, and loss coefficient η_e of a uniform material having the same volume and anchorage points. The second type of unit provides a particularly useful way for predicting the effects of adding a surface addition to members.

The experimental results on several test configurations provide a good check for the theory.

Both the theoretical and experimental results indicate that this new configuration is capable of dissipating very large damping energy. Very large equivalent loss moduli E''_e can be realized (the values for the test configurations were about 4×10^6 psi). Illustrations included in the paper indicate that for many conditions of engineering interest the new configuration is capable of dissipating significantly more energy than conventional free or constrained layer treatments.

VIII. REFERENCES

1. Oberst, H. "Uber die Dampfung der Biegeschwingungen dunner Bleche durch fest haftende Belage," Acustica 2, Akustische Beihefte 4, 181-194 (1952). (A translation has been available from H. L. Blachford, Inc., 7531 Lyndon Avenue, Detroit, Michigan.)

2. Kerwin, E. M. Jr., "Macromechanisms of Damping in Composite Structures," to be published as a STP publication on 1964 Symposium on Internal Friction, Damping, and Cyclic Plasticity Phenomena in Materials, American Society for Testing and Materials, 1965.

3. Hamme, R. N., "Vibration Control by Applied Damping Treatments," Section 37 (Vol. 2) Shock and Vibration Handbook, C. M. Harris, C. E. Crede, Eds., McGraw-Hill Book Company, New York, 1961.

4. Ross, Donald, Ungar, Eric E., Kerwin, E. M. Jr., "Damping of Plate Flexural Vibrations by Means of Viscoelastic Laminae," Structural Damping, pp 49-87, The American Society of Mechanical Engineers, 1959.

5. Ungar, Eric E., "Highly Damped Structures," Machine Design, pp 162-168, February 14, 1963.

6. Baldo, Antonio F., "Dampers," Section 34, Mechanical Design and Systems Handbook, pp 34-1 to 34-22, McGraw Hill Publishing, 1964.

7. Whittier, James S., The Effects of Configurational Additions Using Viscoelastic Interfaces on the Damping of a Cantilever Beam, WADC Technical Report 58-568, Wright Air Development Center, Wright-Patterson Air Force Base, Ohio, May, 1959.

8. Torvik, P. J. and Lazan, B. J., A Corrugated Addition for Increased Damping in Flexure, AFML TR 64-373, Air Force Materials Laboratory, Research and Technology Division, Wright-Patterson Air Force Base, Ohio, January, 1965.

9. Lazan, B. J., "Damping Properties of Materials and Material Composites," Applied Mechanics Reviews, Vol. 15, No. 2, pp 81-88, February, 1962.

10. de Bruyne, N. A., "The Strength of Glued Joints," Aircraft Engineering, April, 1944.

11. Avery, Carlos P., An Investigation of Longitudinal Shear Distribution and Damping in a Viscoelastic Adhesive Lap Joint, WADD Technical Report 60-687, Wright Air Development Division, November, 1960.

APPENDIX A

REDUCTION OF Δ_t TEST DATA FOR η_c AND k''_j

A.1 Values of Storage and Loss Moduli.

The moduli for the test configuration (see Figure 12) may be calculated from Equations (3.31) and (3.32) by inserting the following values for the configuration used in the test program: $m = 0.002"$, $t = 0.006"$, $G' = 15.5$, $G'' = 13.2$ and $E = 3 \times 10^7$ lbs/in^2. For $\ell = 2"$, this leads to values of $k'_j = 1.39 \times 10^4$ and $k''_j = 8.52 \times 10^3$. For $\ell = 4"$, $k'_j = 1.87 \times 10^4$ and $k''_j = 6.30 \times 10^3$.

A.2 Estimation of the Anchor Length

Length L is the distance between the two points p and g of effective anchorage (see Figure 11). For the configuration having $\ell = 2"$ each end rigidly adhered to the member is 2" long (overall length of configuration is 6"). If the 2" anchored ends behave like an integral part of the structural member (and planes perpendicular to the neutral axis remain planes), the points to which the bands are effectively anchored are located at points h and w in Figure 12. In this case L equals 2". If instead the bands in the anchored rigid are assumed to be rigid (and shear strain is allowed to occur in the structural adhesive), the effective anchor points p and q are located midway between end points g and h and points w and y, respectively. Under these circumstances L equals 4". Actual measurements indicate that the effective length L is some distance between these two extremes, actually about 3".

For the configuration having $\ell = 4"$, the anchor length L lies between 4" and 5", and actual measurements indicate that L is 4.5.

Substituting these values of L in Equations (4.12) and (4.13) the values for E'_e and E''_e for each configuration may be calculated, and these are tabulated in Table II.

A.3 Stored Energy U_s in System.

The total stored energy U_s in the testing system is

$$U_s = U_b + U_c + U_p \qquad \text{(A-1)}$$

where:

U_b = strain energy in the test beam.

U_c = strain energy in the treatment attached to the beam.

U_p = potential energy in the pendulum

These energies are expressed below in terms of y_e, the deflection of the lower end of the test beam as shown in Figure 19.

Strain Energy U_b in Beam Test.

The beam shown in Figure 15 is idealized to that shown in Figure 18 for the purposes of this calculation. Since the beam is aluminum $E_a = 12. \times 10^6$ lbs/in^2. Referring to Figures 18 and 19, the following can be defined.

y_e = deflection of the end of the test beam (at x = 7").

p = radius of curvature of the neutral axis
$= 24.5/y_e$.

y_{na} = depth of the neutral plane from the surface of the beam to which the treatment is attached.

Since the aluminum beam is tapered, the location of the neutral axis varies with position along the x axis of the beam. However, to simplify calculation the position of the neutral axis is assumed constant and equal to that for an aluminum beam having a constant width of 1.58". For a treatment 1 inches wide and d inches thick, and considering equilibrium (moments of stress about the neutral axis must be zero), the following equation follows:

$$1.58\, E_a \int_{y=o}^{(.187-y_{na})} y\,dy = 1.58\, E_a \int_{y=o}^{y_{na}} y\,dy + E'_e \int_{y=y_{na}}^{(y_{na}+d)} y\,dy$$

$$y_{na} = \frac{.0555E_a - d^2E'_e}{.592\, E_a + 2dE'_e} \qquad (A.2)$$

Considering this shift in the neutral axis the strain energy in the test beam is:

$$U_b = \int_{vol} (\tfrac{1}{2} E_a \epsilon^2)\,dv = \int_v \tfrac{1}{2} E_a \frac{y^2}{\rho^2}\,dv = \frac{E_a}{2\rho^2} \int_{x=o}^{x=7} \int_{y=(y_{na}-.187)}^{y=y_{na}} \int_{z=-(1-.06x)}^{z=1-.06x} y^2\,dz\,dy\,dx$$

$$= \frac{y_e^2\, E_a}{2(24.5)^2} \int_{x=o}^{7} \int_{y=(y_{na}-.187)}^{y_{na}} 2y^2\,(1 - .06x)\,dy\,dx$$

$$= \frac{y_e^2 \; E_a}{(24.5)^2} \int_{x=o}^{7} \frac{1}{3} \left[y_{na}^3 - (y_{na} - .1875)^3 \right] (1 - .06x)\,dx$$

$$= .0030 \; E_a (.562\, y_{na}^2 - .105\, y_{na} + .0066)\, y_e^2 \qquad \text{(A-3)}$$

Strain Energy U_c in Configuration.

The treatment is regarded as a homogeneous material with properties E_e' and E_e'' of length L, breadth b, and height d extending from y_{na} to $(y_{na} + d)$ above the neutral axis. Its strain energy is:

$$U_c = \int_{vol} \frac{1}{2} E_e' \varepsilon^2 d(vol) = \frac{1}{2} E_e' \frac{y_e^2}{\rho^2} \int_{x=o}^{L} \int_{y=y_{na}}^{(y_{na}+d)} \int_{z=o}^{b} y^2 dx dy dz$$

Integrating and substituting for ρ:

$$U_c = \frac{E_e' bLd}{6(24.5)^2} (3y_{na}^2 + 3y_{na}d + d^2) y_e^2 \qquad \text{(A-4)}$$

Potential Energy U_p in Pendulum.

Figure 19 shows a schematic diagram of the pendulum in its deflected position. The energy associated with the pendulum effect is equal to the mass M_p of the pendulum multiplied by the change in height of center of mass of the pendulum during the oscillation. Thus,

$$U_p = M_p \; z = M_p \left[h + r \; (1 - \cos \theta) \right]$$

Assuming for small angles $\tan \theta \approx \frac{dv}{dx} \approx \theta$, and the elevation of the center of mass is:

$$h = 7 - \int_{o}^{7} \cos \left(\frac{dv}{dx}\right) dsc$$

where

$$\cos \left(\frac{dv}{dx}\right) \approx 1 - \frac{1}{2} \left(\frac{dv}{dx}\right)^2, \; \frac{dv^2}{dx^2} = \frac{1}{\rho}, \text{ and } \frac{dv}{dx} = \frac{x}{\rho} \; ,$$

$$h = 7 - \int_0^7 \left(1 - \frac{1}{2}\left(\frac{x}{\rho}\right)^2\right) dx = \frac{7^3}{6\rho^2}$$

$$1 - \cos\theta = 1 - \left(1 - \frac{7^2}{2\rho^2}\right) = \frac{7^2}{2\rho^2}$$

Therefore, $U_p = M_p \left(\frac{7^3}{6\rho^2} + r \frac{7^2}{2\rho^2}\right)$

$$U_p = 37.85\, y_e^2 \qquad \text{(A-5)}$$

Results.

The values of U_b, U_c, U_p and y_{na} for the different treatment configurations, calculated using the above equations, are tabulated in Table II.

A.4 Damping Properties of the Configuration and the System.

The energy dissipation in the treatment is:

$$D_c = \int_{vol} \pi E_e'' \epsilon^2 \, d(vol) = 2\pi \frac{E_e''}{E_e'} U_c = 2\pi \frac{k_j''}{k_j'} U_c \qquad \text{(A-6)}$$

Therefore, $(k_j'')_{exp.} = k_j' \frac{U_s}{U_c} (\eta_s)_{exp.}$ (A-7)

The experimentally determined values of η_s are tabulated in Table I. The values of k_j'' calculated from the experimental results are plotted in Figure 13.

TABLE I

COMPARISON BETWEEN VALUES OF THE LOSS COEFFICIENT η_s OF THE TEST CONFIGURATION: - (a) VALUES OBSERVED EXPERIMENTALLY AND (b and c) VALUE PREDICTED BY THE THEORY

Test Configuration		Values of η_s		
		a) Determined Experimental Values	Values Predicted by Theory	
			b) Using E''_e Approach	c) Approximate Summation Process
ℓ	n			
2	4	0.031	0.031	0.031
2	2	0.017	0.014	0.014
2	1	0.010	0.007	0.008
4	2	0.028	0.021	0.027

TABLE II

MEASURED AND CALCULATED VALUES FOR THE TEST CONFIGURATION AND SYSTEM

Configuration		E'_e	E''_e	y_{na}	U_b	U_p	U_c	D_c	η_c
ℓ	n								
2	4	4.19	2.55	.090	59.2	37.8	5.1	19.8	.0308
2	2	3.49	2.13	.091	59.1	37.8	2.2	8.6	.0138
2	1	2.62	1.60	.092	59.0	37.8	1.0	4.1	.0066
4	2	7.02	2.36	.089	59.5	37.8	6.4	13.6	.0210
		Multiply by 10^6			Multiply by y_e^2				

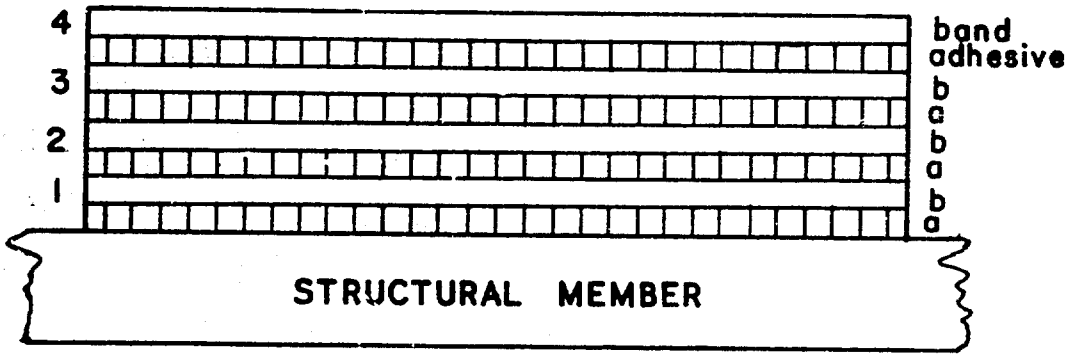

(a) UNSTRAINED CONDITION

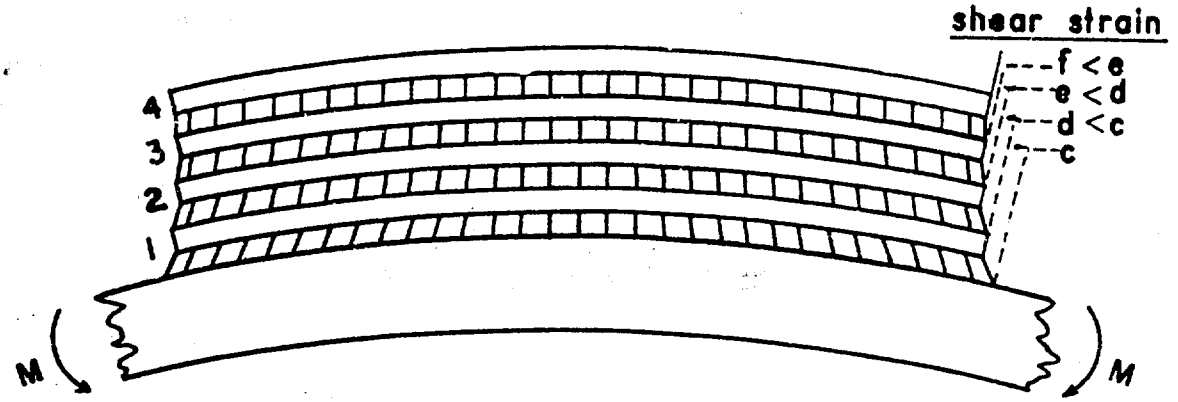

(b) STRAINED CONDITION

Figure 1 Conventional Damping Tape Treatment.
Multiple Band (4 Layer) Configuration

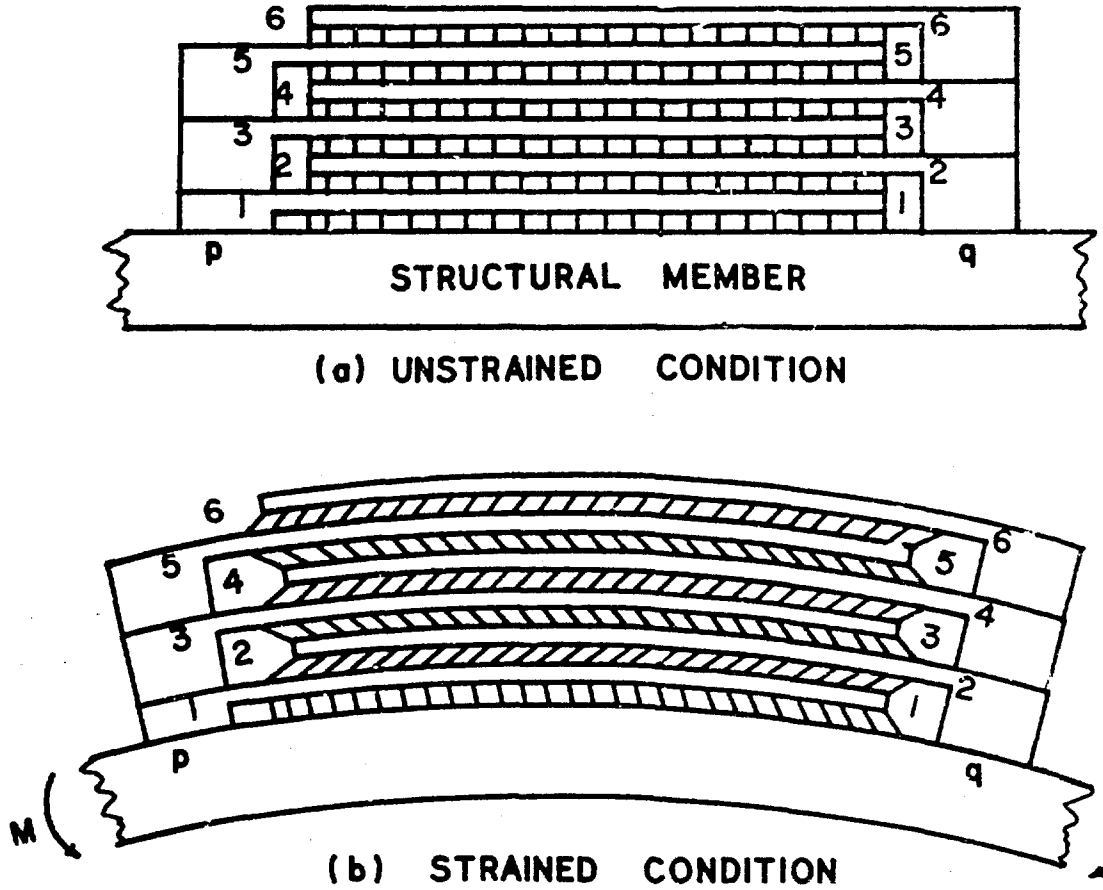

Figure 2 Alternately Anchored Multiple-Band Treatment Configuration Having 5^{+} Layers.

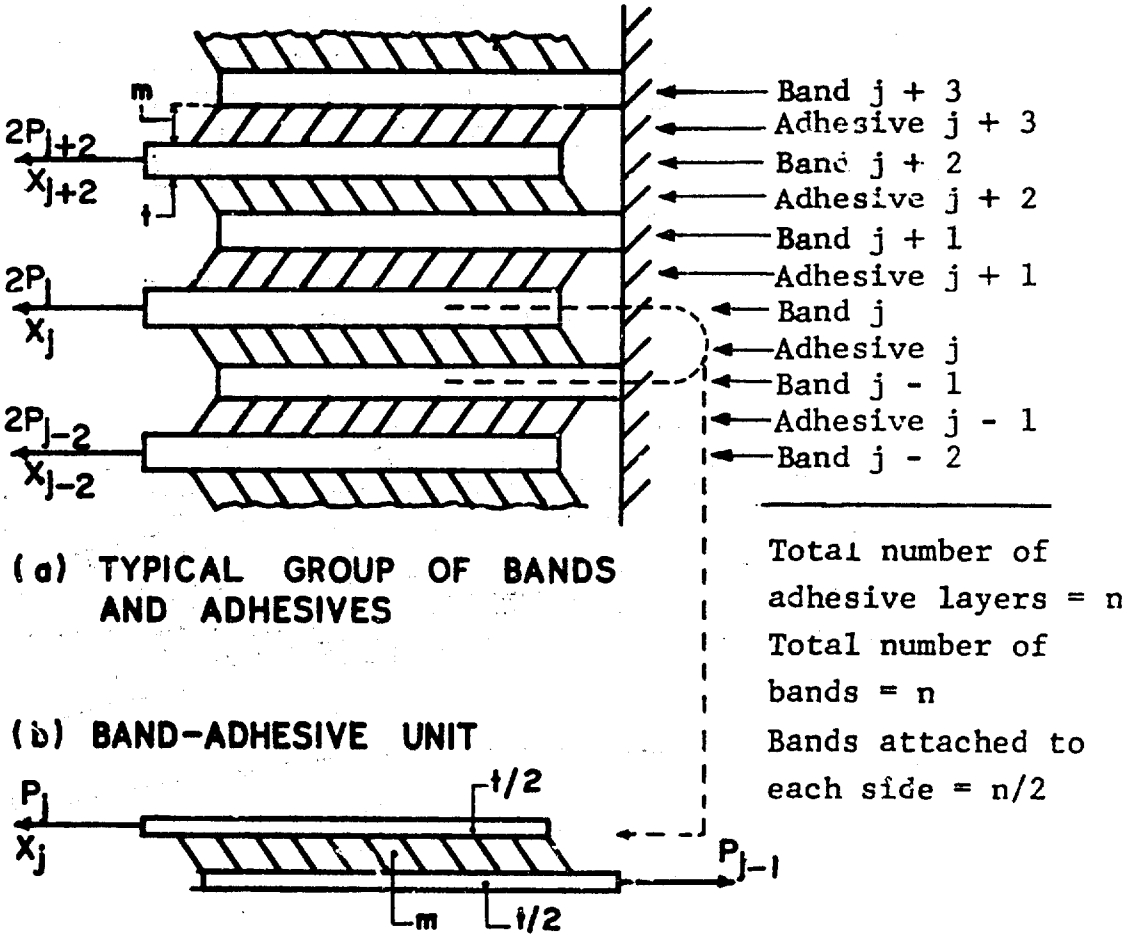

Figure 3 Definition of the Band-Adhesive Unit.

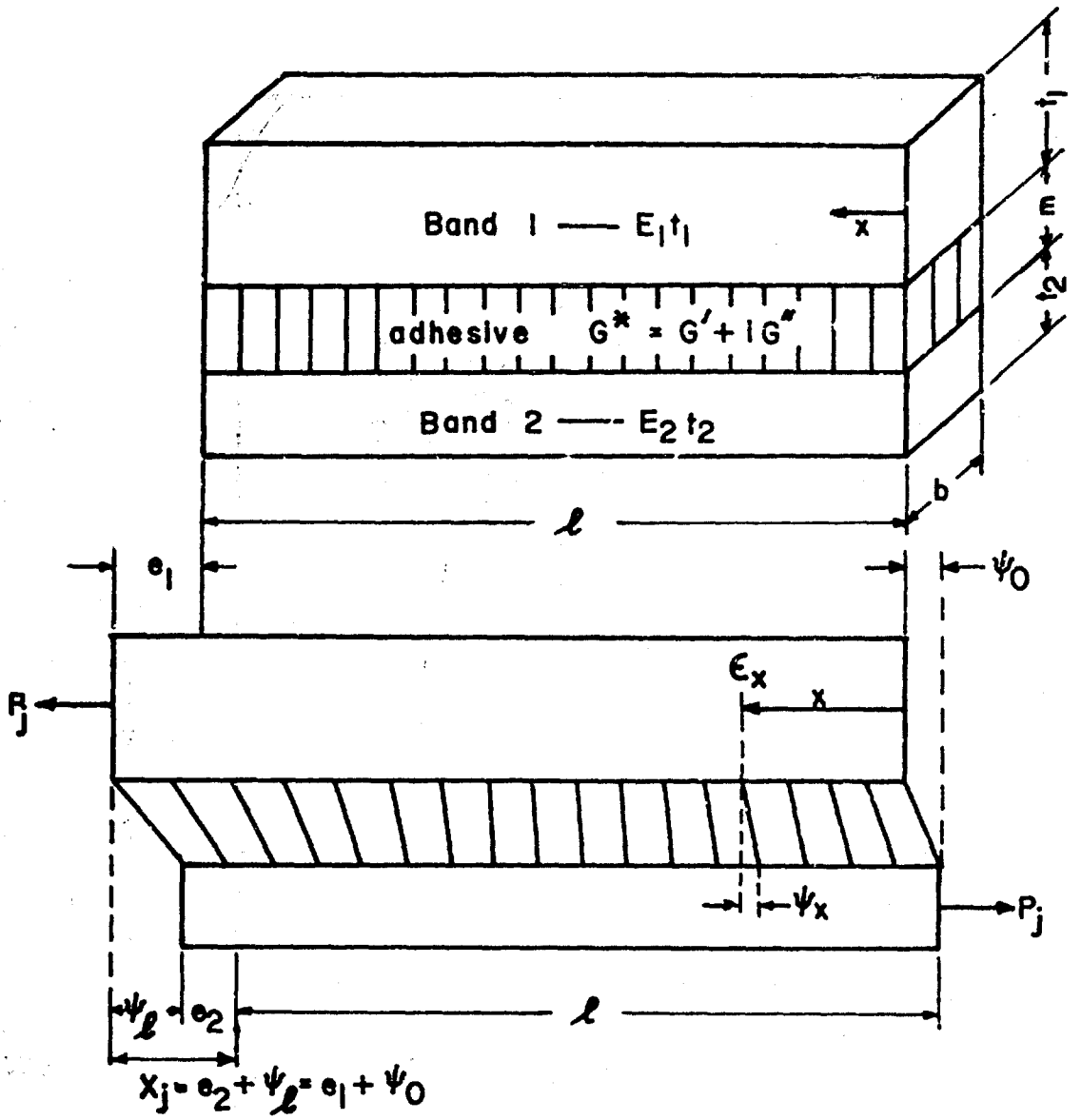

Figure 4 Geometry and Strain Definition for the Band-Adhesive Unit.

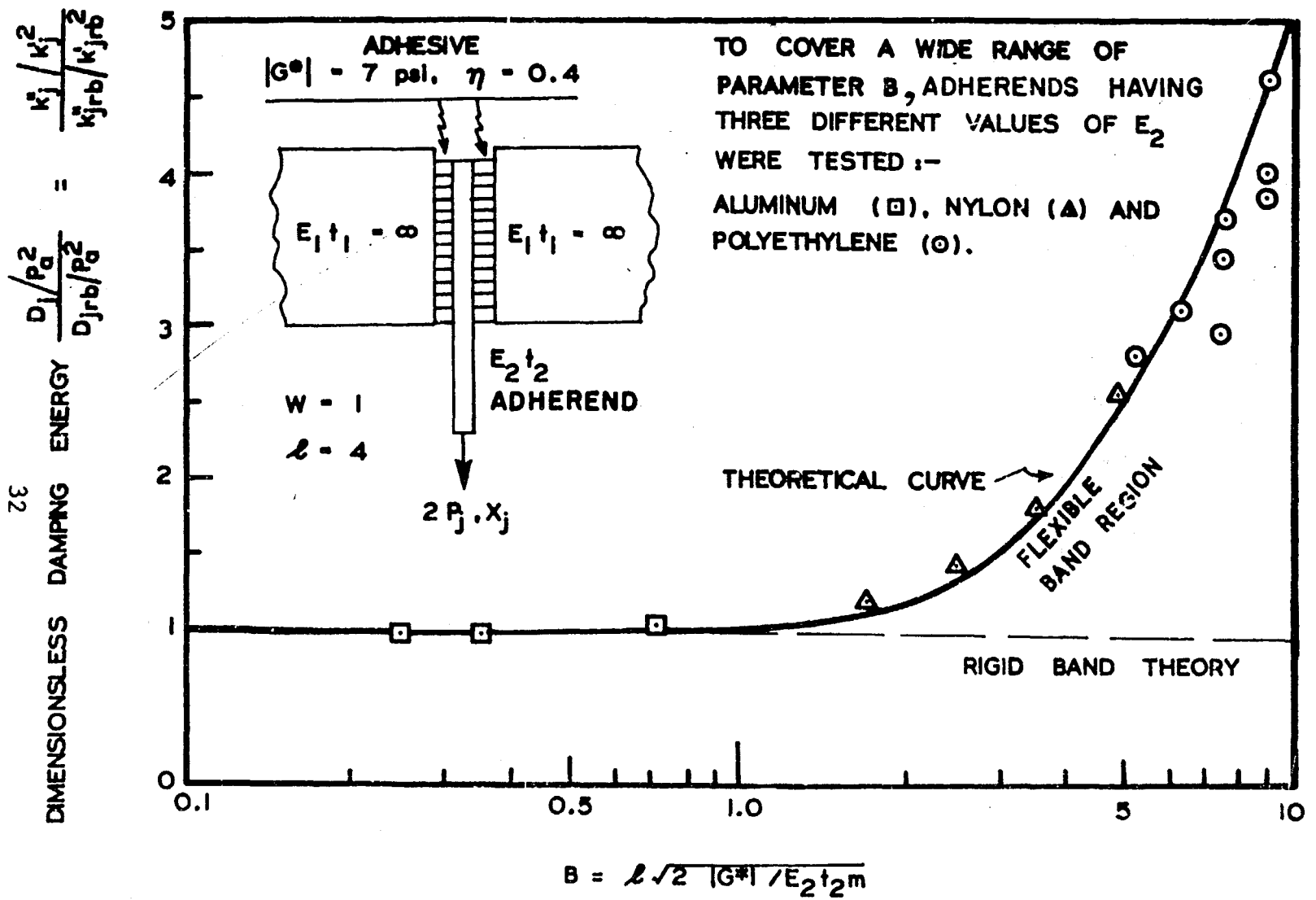

Figure 5 Comparison Between Theoretical Curve and Experimental Data for Double Band-Adhesive Unit Having W = 1.

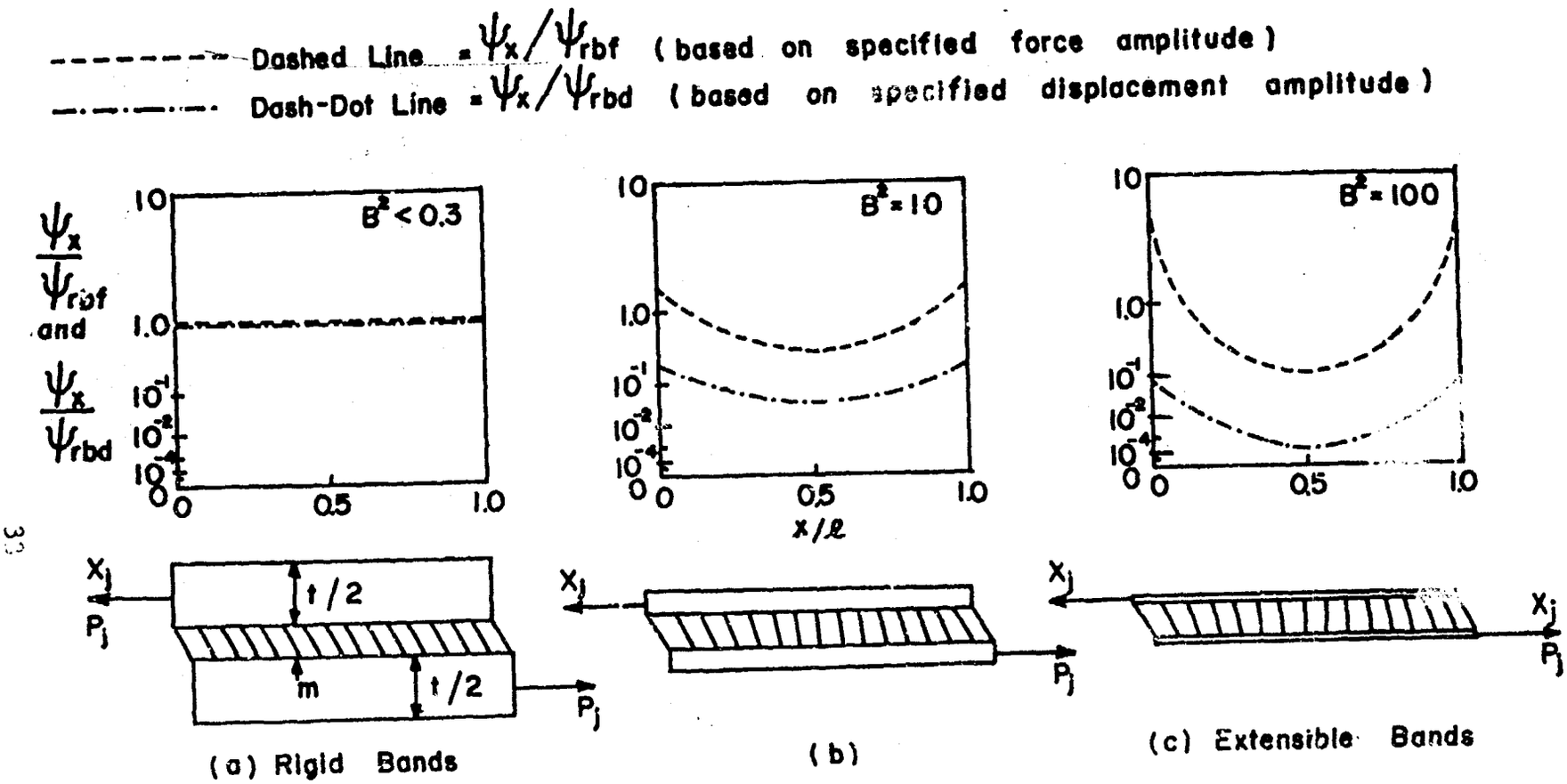

Figure 6 Effects of Parameter B on Shear Distribution in Adhesive for Equal Band Case ($W^2 = 2$). $\eta = 0.4$ and $G^* = 7$.

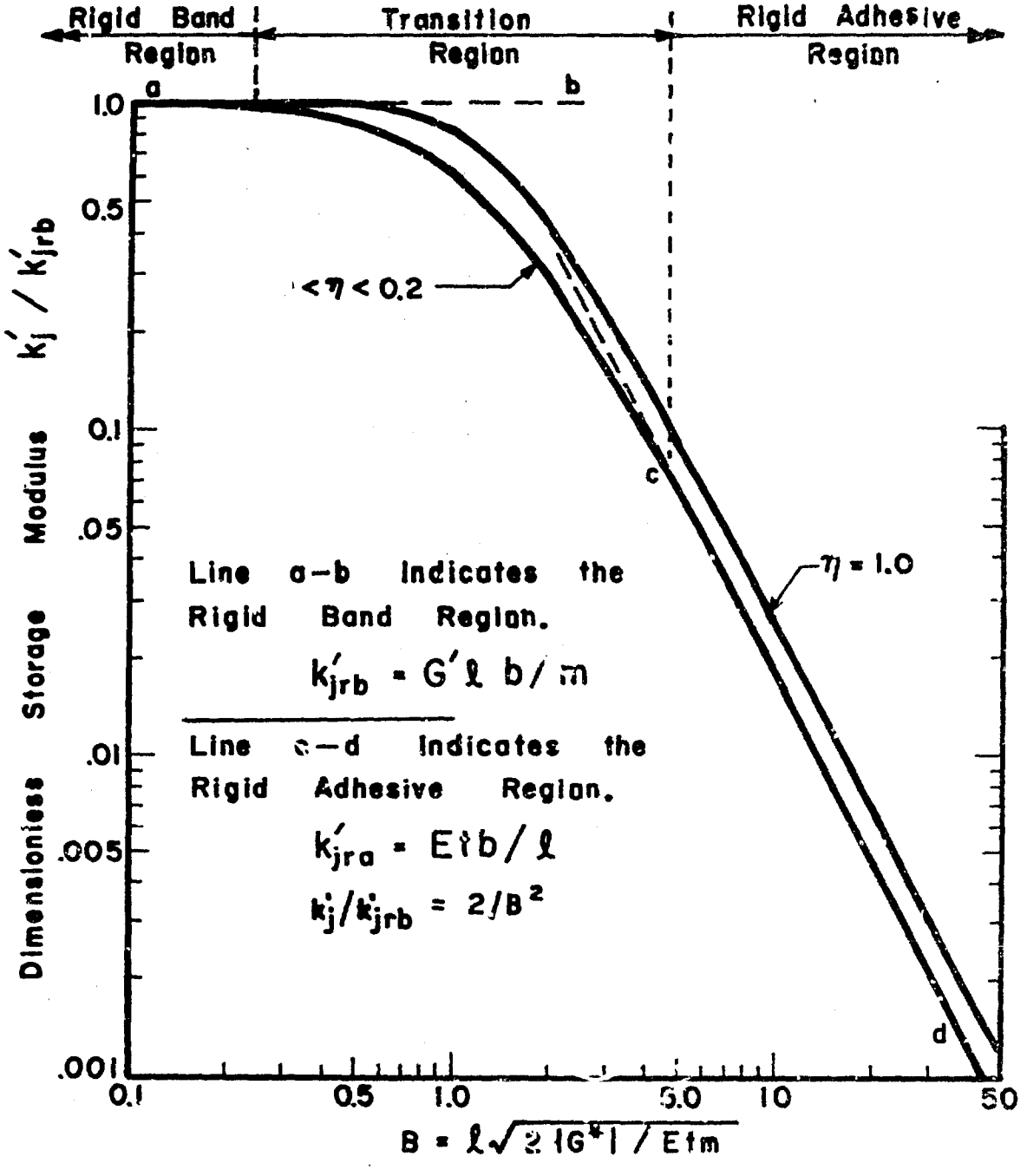

Figure 7 Effect of Parameter B on Dimensionless Storage Modulus of the Band-Adhesive Unit Having Equal Bands.

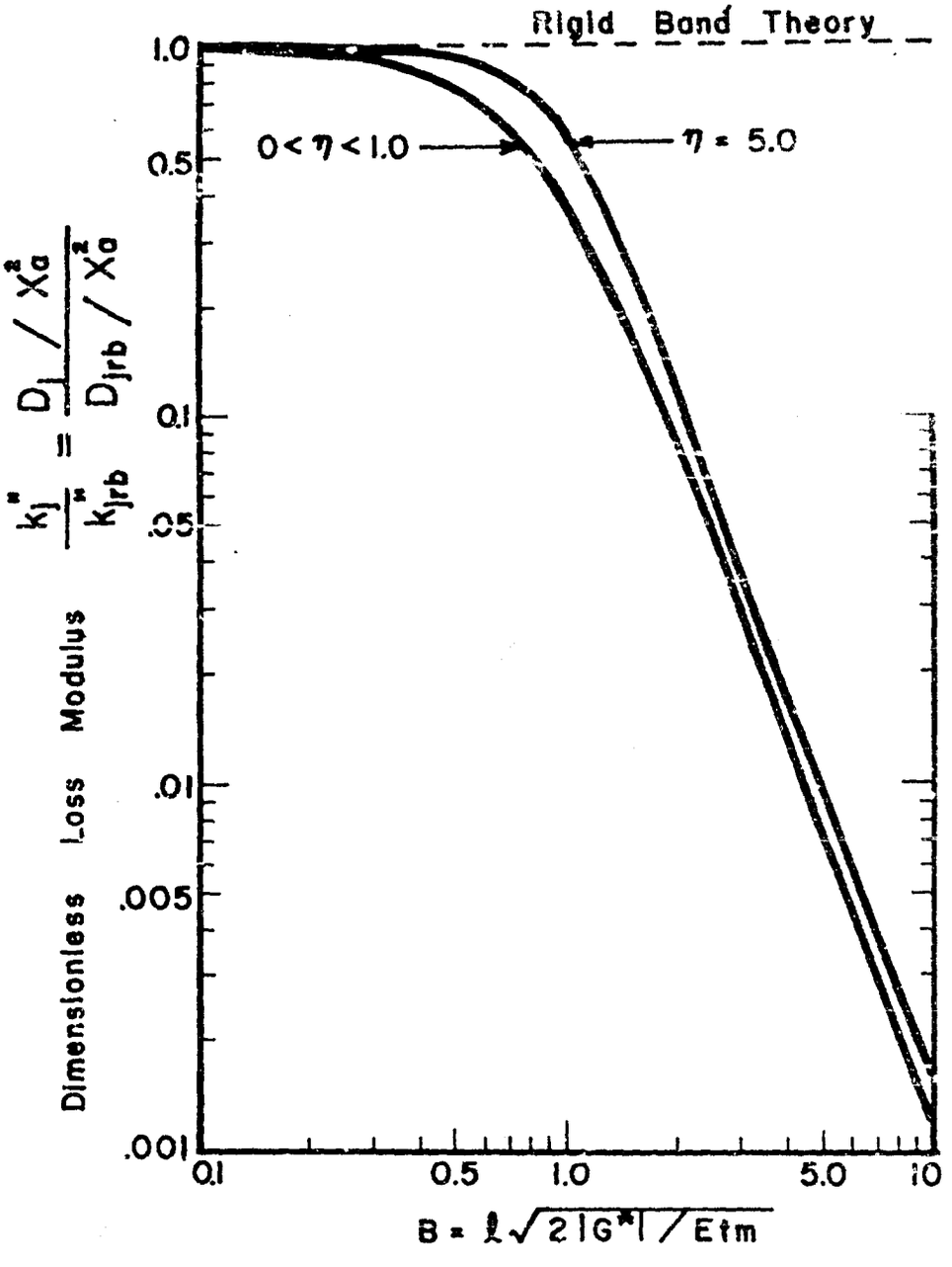

Figure 8 Effect of Parameter B on the Dimensionless Loss Modulus of the Band-Adhesive Unit Having Equal Bands.

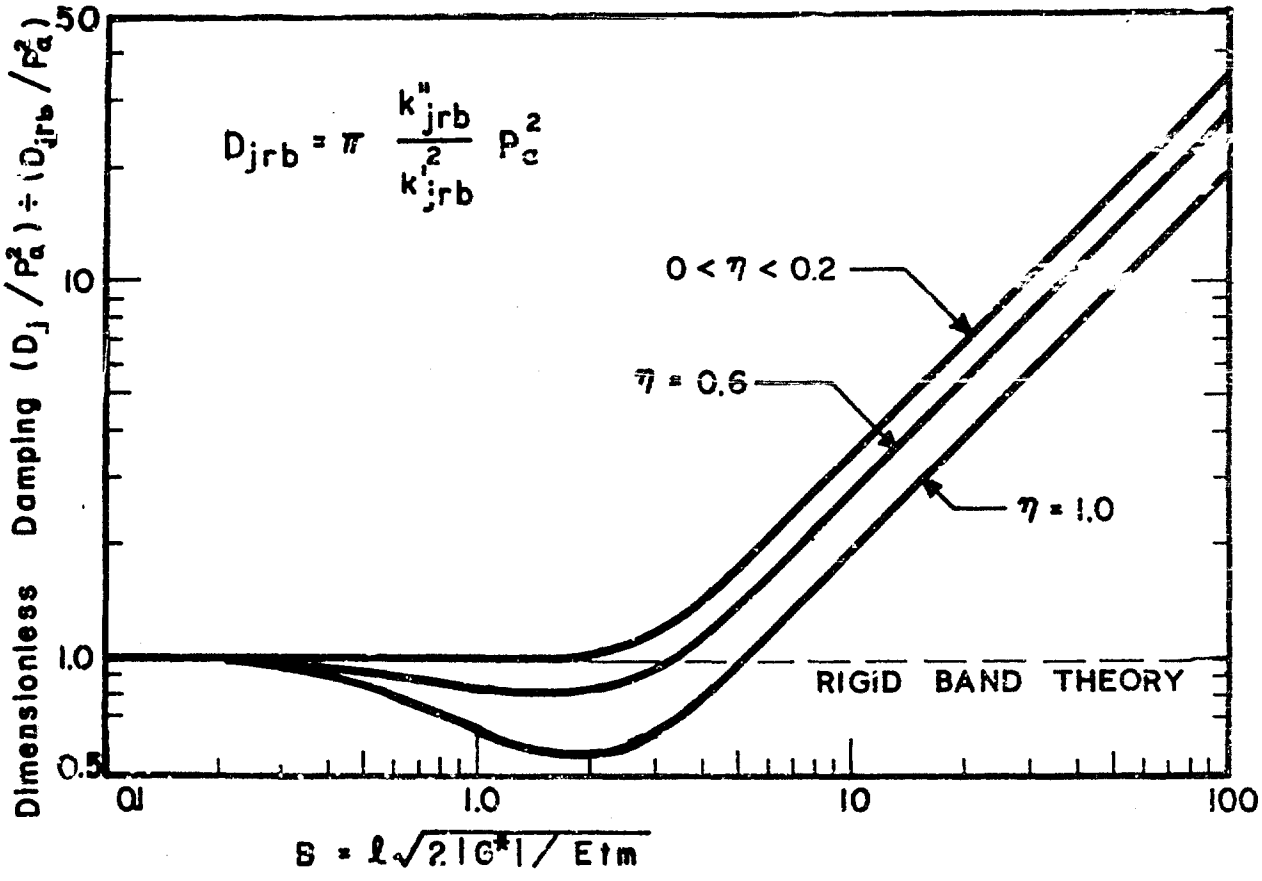

Figure 9 Effect of Parameter B on Dimensionless Damping Energy at a Specified Force Amplitude.

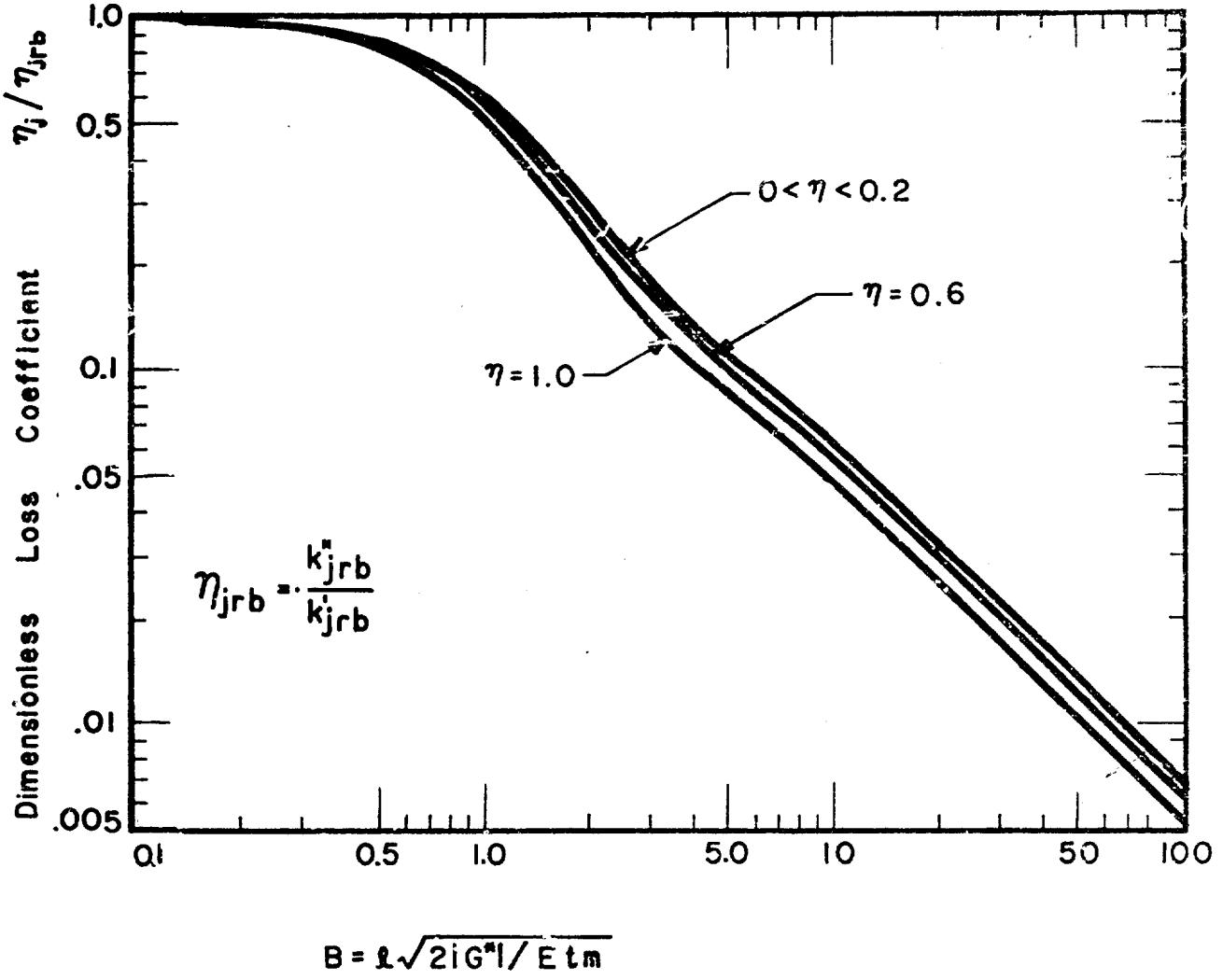

Figure 10 Effect of Parameter B on Dimensionless Loss Coefficient.

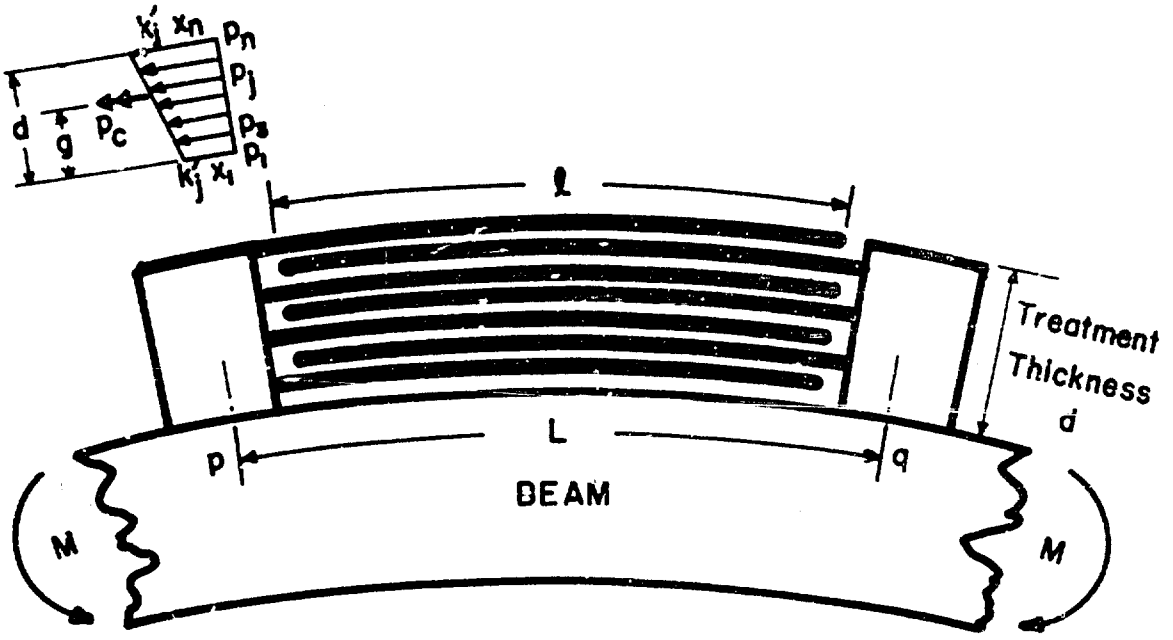

Figure 11 Thick Treatment Geometry and Displacement Distribution Under Flexure.

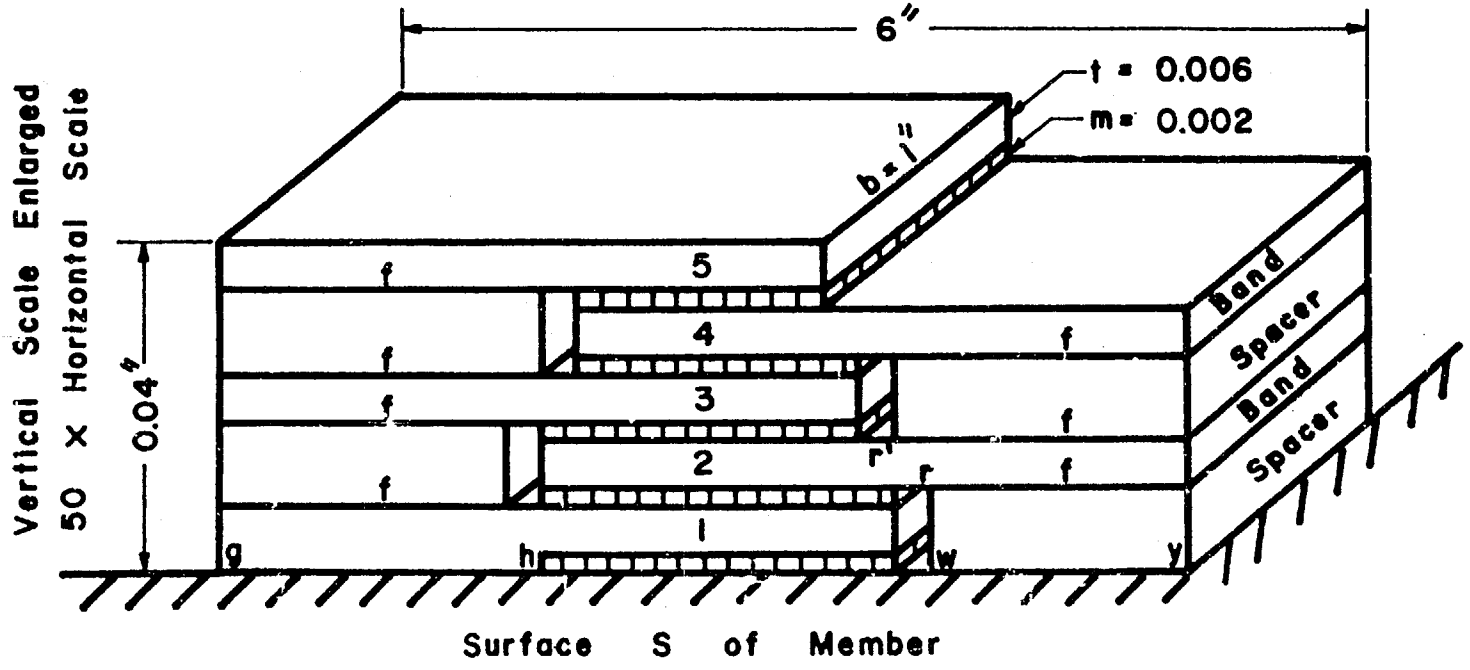

Figure 12 Multiple-Band Configuration Used in Test Program. Band Surfaces f Joined by Structural Adhesive. Configuration Joined to Surface S of Member by Structural Adhesive at Interfaces g-h and w-y.

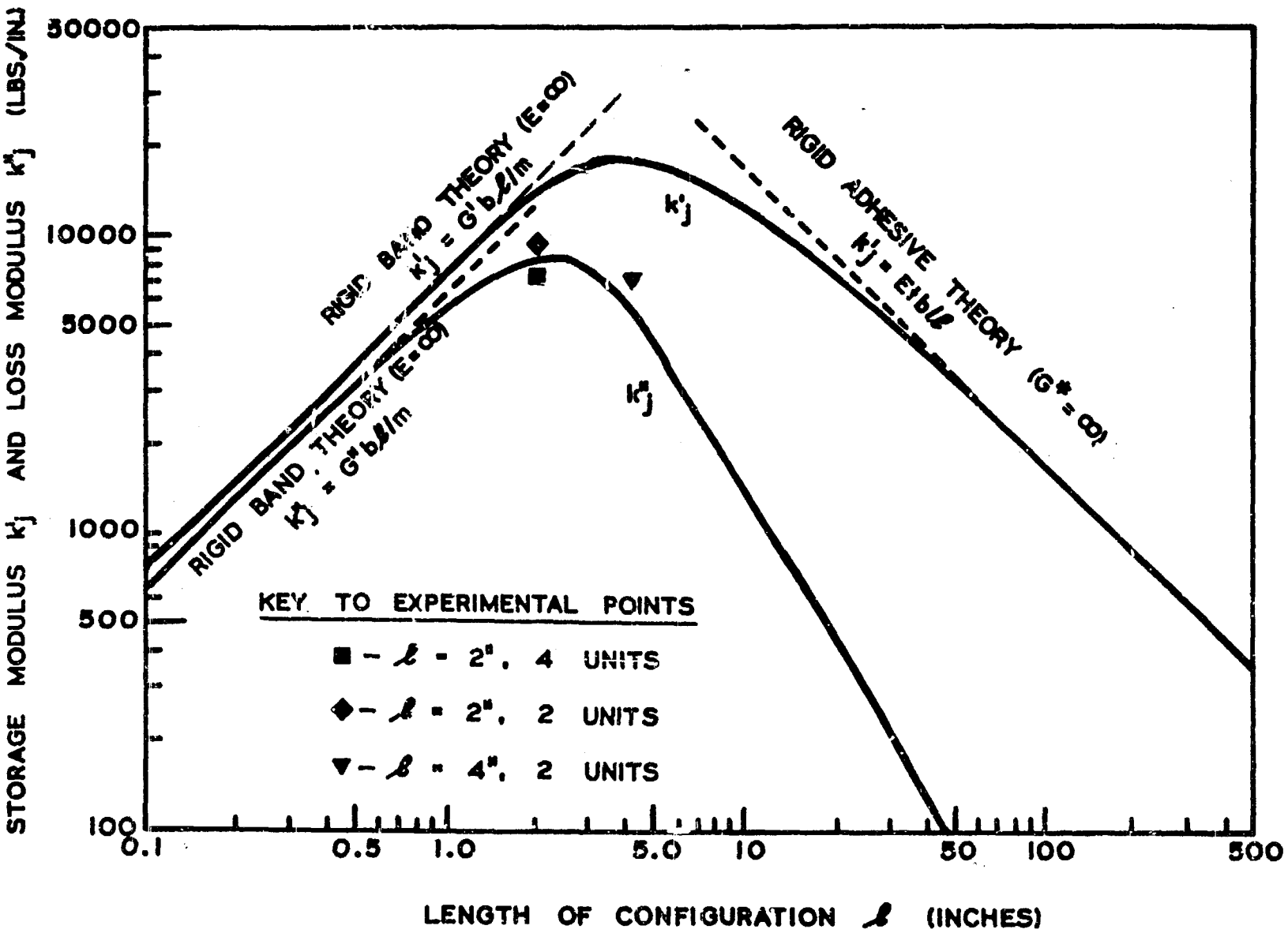

Figure 13 Theoretical Curves for Storage and Loss Modulus of Test Configuration as a Function of Length ℓ. Points Show Experimental Values.

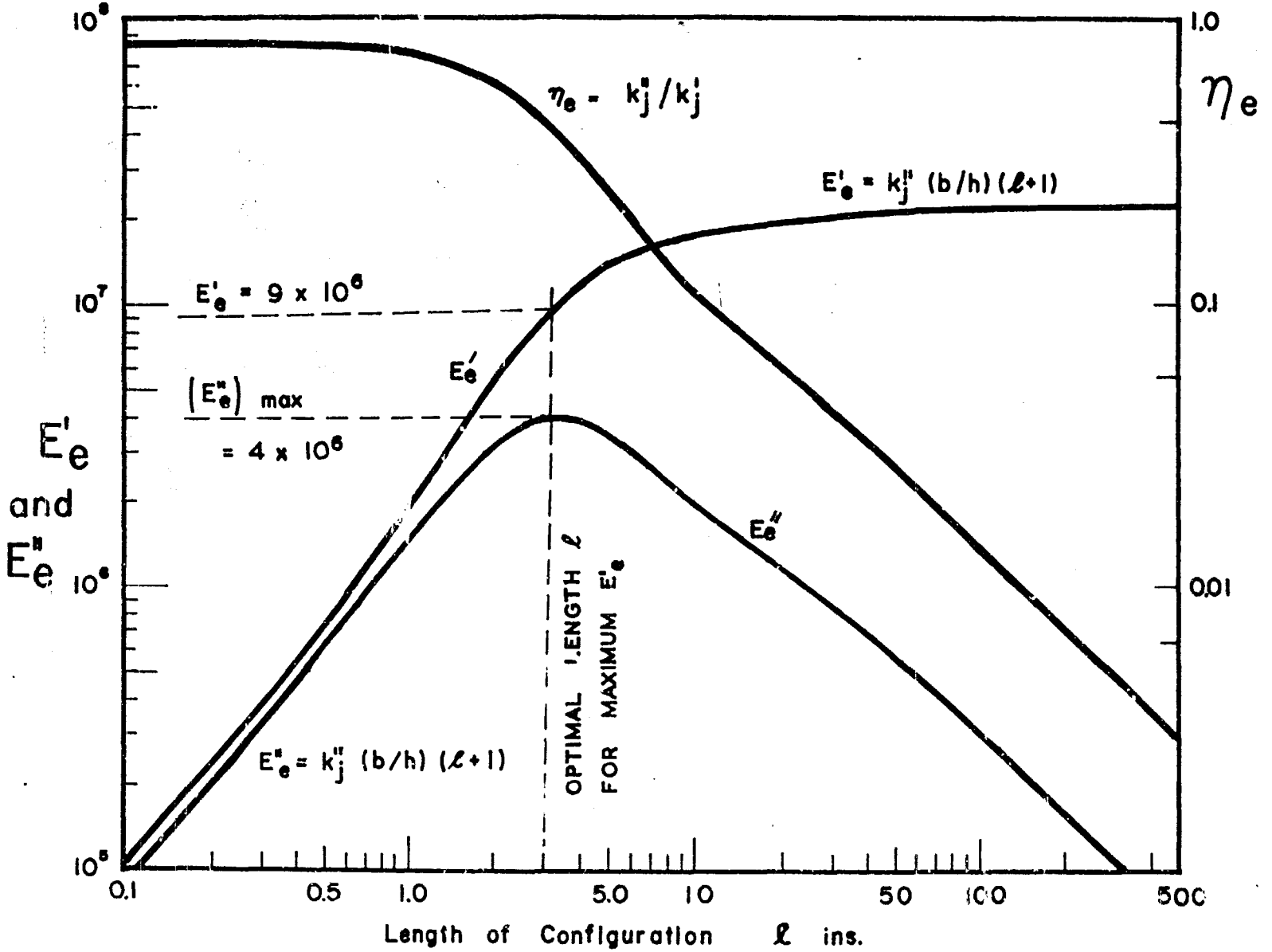

Figure 14 Theoretical Curves Showing the Equivalent Storage and Loss Moduli and the Loss Coefficient of Test Configuration for $L = \ell + 1$.

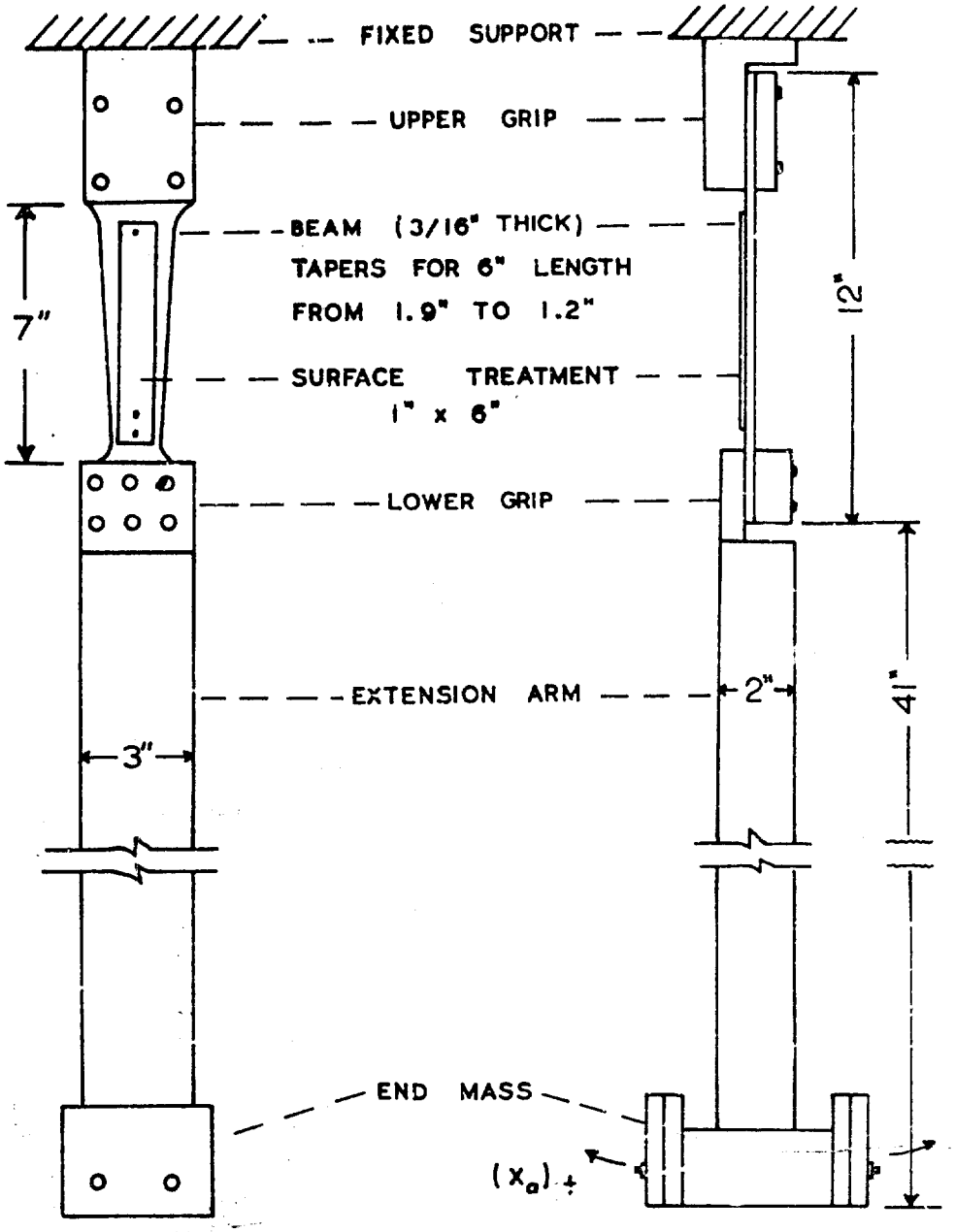

Figure 15 Schematic of Vibration Decay Test Set-Up.

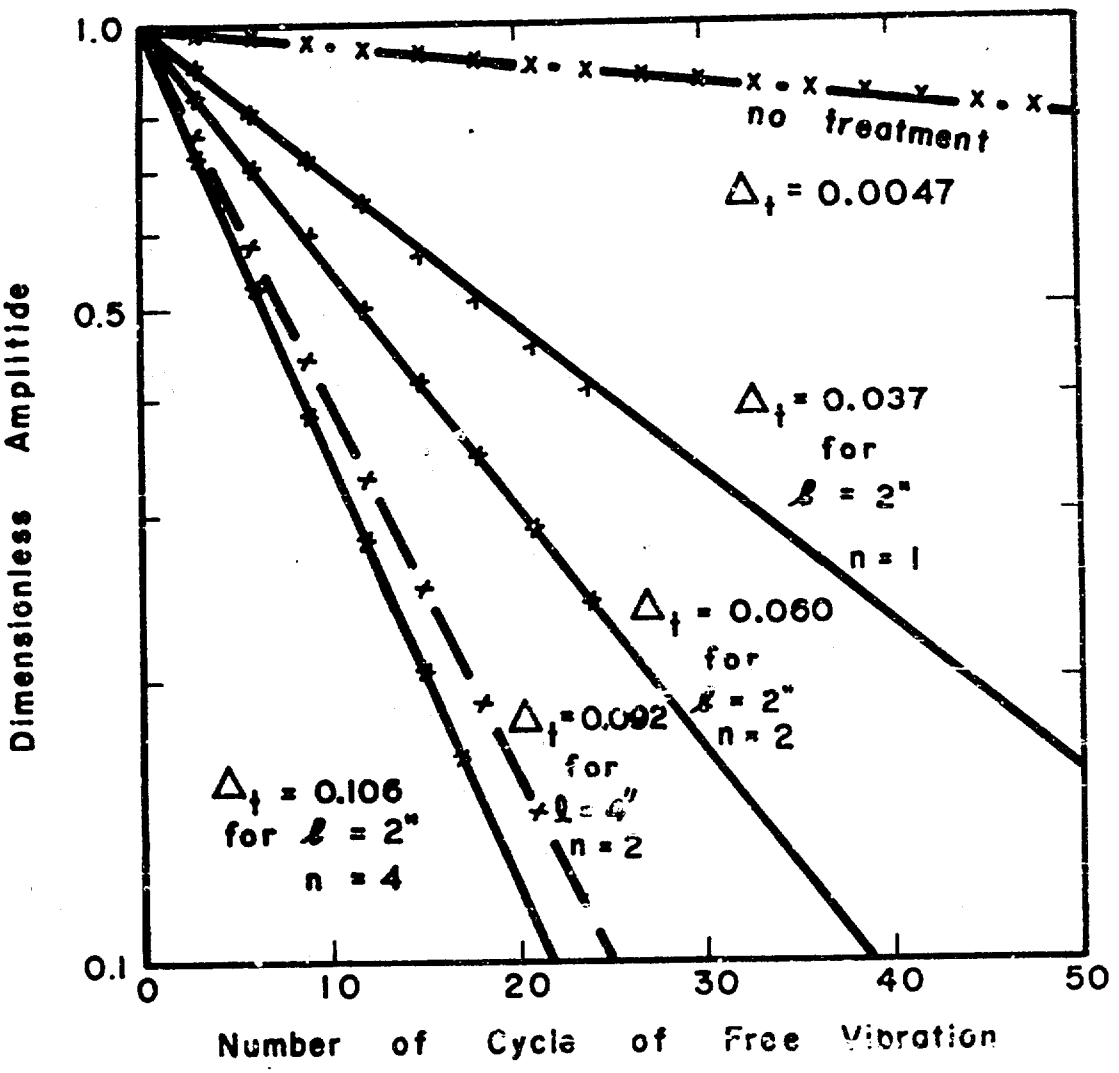

Figure 16 Experimental Decay Curves and Values for Logarithmic Decrement Δ_t for Test Beam with No Treatment and Four Types of Surface Treatments.

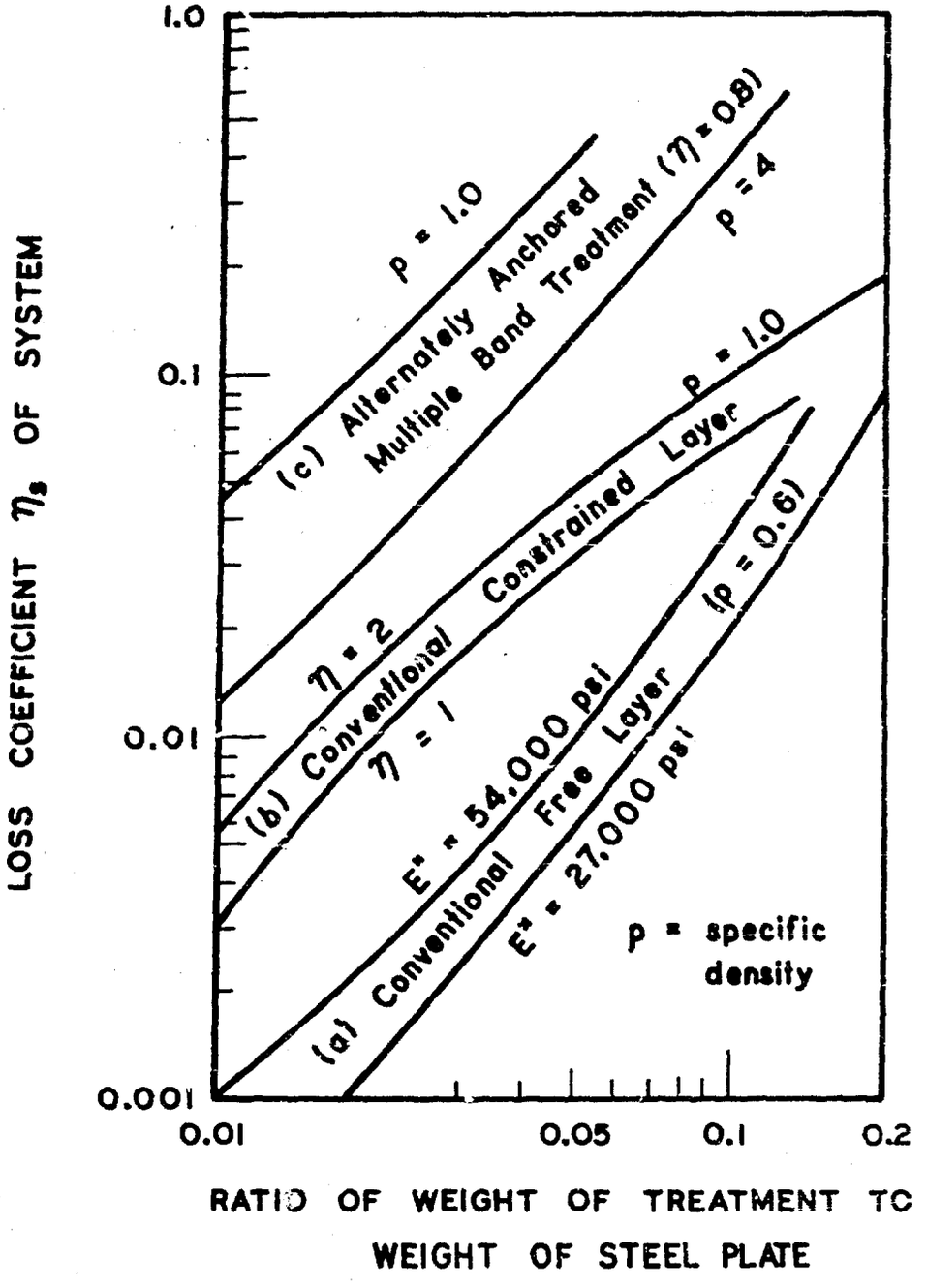

Figure 17 Relative Effectiveness of Free Layer, Constrained Layer, and Alternately Anchored Multiple-Band Treatment. Maximum η_s Shown for (a) and (b), η_s for (c) not Maximized. (see References 2 and 5)

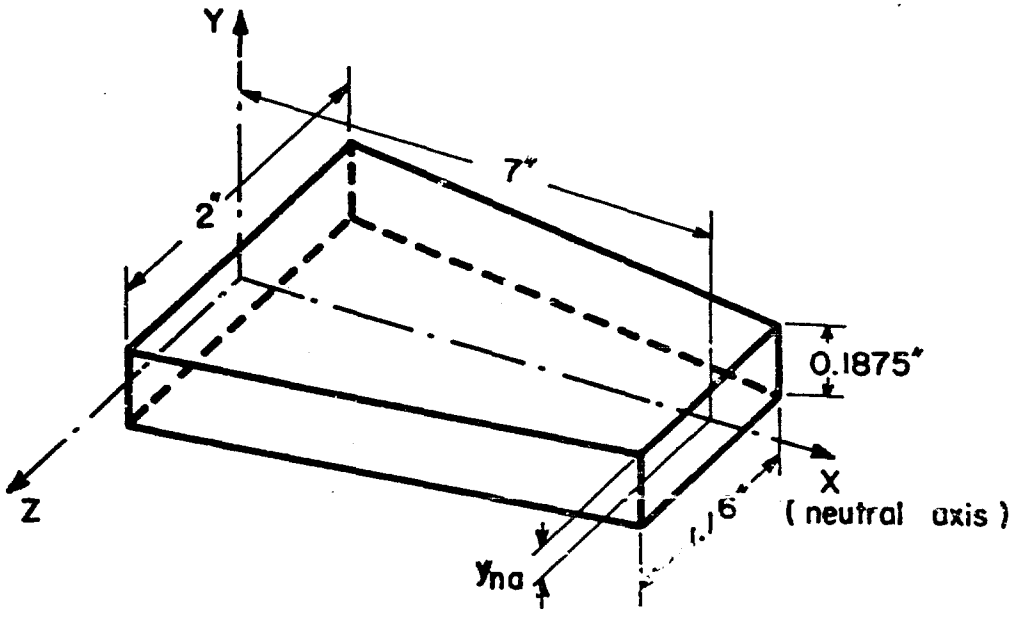

Figure 18 Idealization of Aluminum Beam to Which the Treatment was Attached.

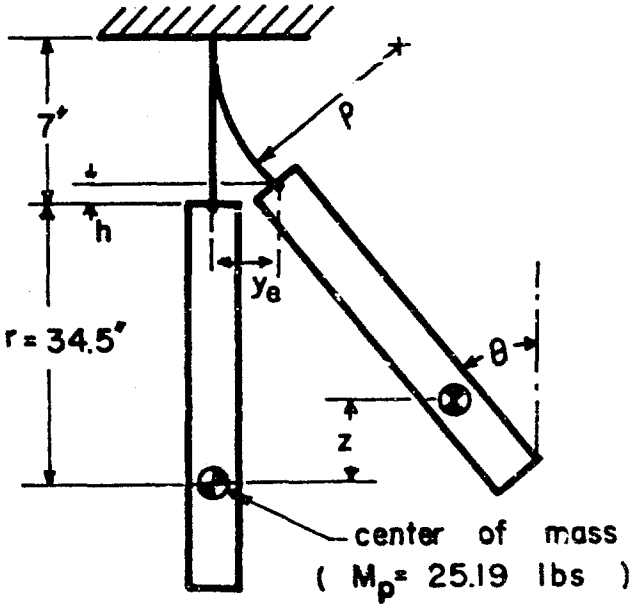

Figure 19 Idealization of the Pendulum System.